5-10-2018

Geometric Properties and a Combinatorial Analysis of Convex Polygons Constructed of Tridrafters

Trevor Nelson

Geometric Properties and a Combinatorial Analysis of Convex Polygons Constructed of Tridrafters

by

Trevor Nelson

A Thesis Submitted in Partial Fulfillment of the Requirements

for the Degree of Master of Science in Applied Mathematics

School of Mathematical Sciences, College of Science

Rochester Institute of Technology

Rochester, NY

May 10, 2018

Committee Approval:

Dr. Matthew Coppenbarger — Date

School of Mathematical Sciences

Thesis Advisor

Dr. Darren Narayan — Date

School of Mathematical Sciences

Committee Member

Dr. Hossein Shahmohamed — Date

School of Mathematical Sciences

Committee Member

Dr. Matthew J. Hoffman — Date

School of Mathematical Sciences

Director of Graduate Programs

Abstract

The aim of this thesis is to show how the use of parity in tandem with the triangular grid as well as a newly introduced and similar method are insufficient to provide proof for why convex regions composed using the full set of shapes known as "proper tridrafters" have a portion shifted in a fashion known as against-the-grain. These two methods are applied in a combinatorial fashion.

Contents

List of Figures

List of Tables

I. Introduction

Since times ancient we as humans have set ourselves apart from other animals by having a curiosity on how things work; even if the mechanism isn't relevant to other branches of science at the time. How might seemingly different things be put together to create a larger whole? We've entertained ourselves with such a concept; often in the form of puzzles. Puzzles allow us to acquire knowledge on how the small individual parts we're given work together to create something larger than the some of those parts. Geometric puzzles, logic puzzles, or even word puzzles can allow us to see how we may approach problems in various fashions as there may be multiple solutions to the same riddle. We see how things that look different can interlock with one another and be similar despite the apparent first impression they may give. With this curiosity, we now have a tremendous amount of geometric puzzles that have been created throughout human existence.

Some puzzles start with a whole and have us create the parts. Haberdasher's puzzle is one of the best known solved puzzles of this kind. We are asked "Can one take an equilateral triangle and dissect it such that the pieces created can be reconfigured into a square?" Henry Dudeney first proposed this question in 1902. After discussion with other mathematicians, an interesting solution was found. Not only can the triangle be dissected, but the triangle may be separated into four "hinged" pieces such that they could be swiveled to create the square solution as shown in Figure 1 [16]. From this alone one may list an infinite number of solutions.

Figure 1: A solution to Haberdasher's puzzle

Geometric puzzles will often make use of polygons for the creation of their individual pieces or a specific polygon as the ending form of the overall goal.

Definition 1. A *polygon* is a bounded region upon a flat plane whose boundary consists of a finite number of line segments, each of finite length, and each line segment intersects with exactly two other individual line segments at endpoints of said line segments. The intersection of the line

segments are *vertices* of the polygon. (E.g. the square has four sides and four vertices; the triangle has three sides and three vertices.)

Jigsaw puzzles will usually form a rectangle when joined together to create the intended solution. Other puzzles make use of the grouping of similar polygons such as McMohan squares and triangles. This puzzle utilize tiles with a color along each edge and each pair of tiles joined alongside edges must match in color. These types of puzzles most often work with congruent polygons which are also often regular such as squares, equilateral triangles, or some other relatively simple shape. We are not limited to this though; see Fredrickson [3] for a comprehensive overview of dissection puzzles.

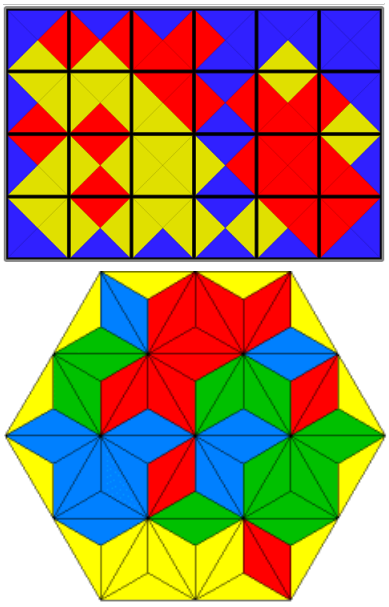

Figure 2: MacMahon square and triangle solution layouts

What of creating other geometrical figures? Tessellations are things that have captivated the attention of people both inside and outside of the mathematical community. Some of these creations are simple enough to observe for anyone to be intrigued upon examining such work. A very famous figure, perhaps the best known, would be M.C. Escher who has drawn the attention of the entire world through his use of the mechanics of isometric relationships. We can demonstrate that tessellating patterns of great complexity still start from a fairly simple foundation. Figure 3 depicts a couple of different layouts of points which may be used to easily

create cells, one comprised of squares and the other of equilateral triangles, that might act as such a foundation.

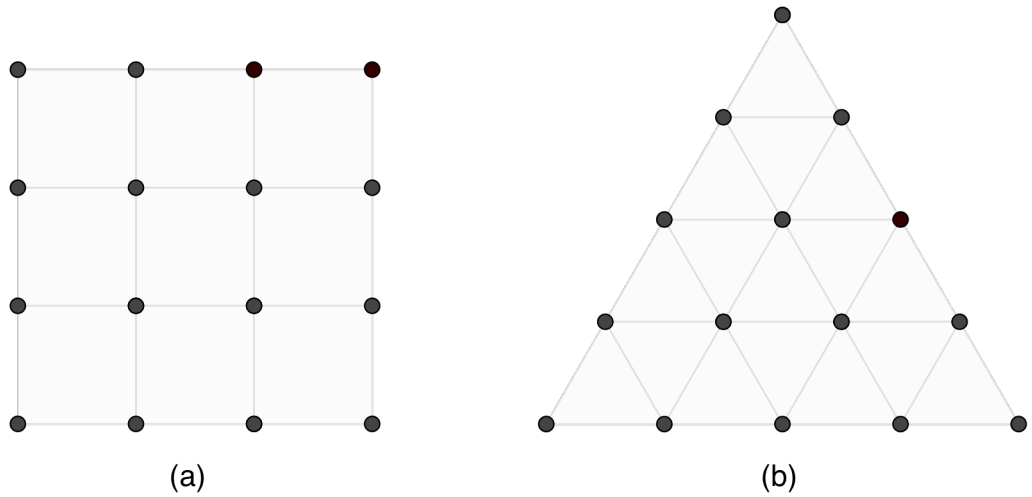

Figure 3: Square and equilateral triangular lattice structures

A *lattice L* can be regarded as a regular tiling of the plane by a primitive cells forming a set of edges. For our purposes, we will only utilize squares and equilateral triangles as our primitive cells. (One more case will be utilized later)

With any particular lattice, we may utilize part of (Figures 4(a) and 5(a)), the whole of (Figures 4(b) and 5(b)), the union of cells (Figure 5(c)), or the union of parts of cells (Figure 4(c)) to create a *base*; an alpha to start with when creating polygons of greater complexity. There are arguably an infinite number of bases that may be created. Schattschneider's work [13] provides a large variety of tessellations created from the varying lattice structures. For this paper however,

we will restrict our usage of lattice structures to squares and equilateral triangles.

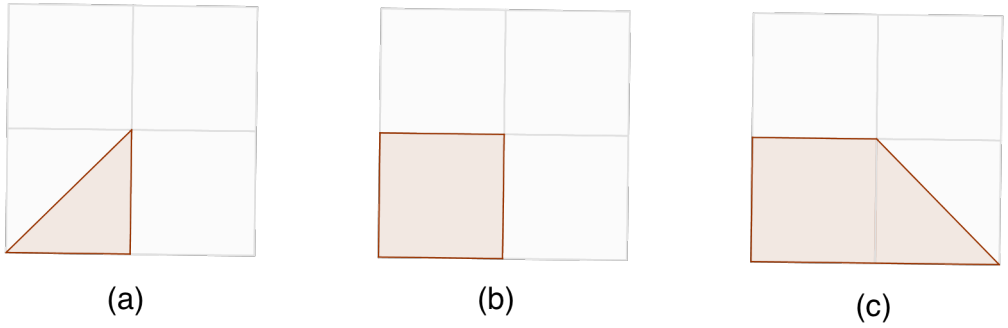

Figure 4: Bases from square lattice

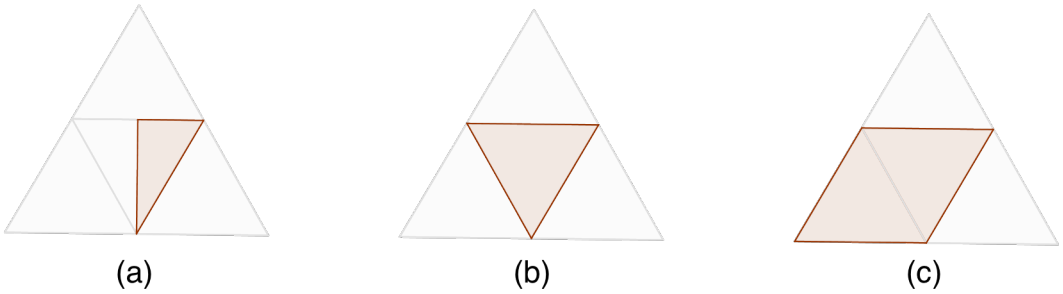

Figure 5: Bases from triangular lattice

Any puzzle involving physical pieces, for many, are the simplest to understand or at least attempt due to their "hands on" nature. We take a set of figures created under a set of rules and create a larger whole often using each element within the set constructed. Tiling puzzles are perhaps the most versatile of these; they have complexities that range from the very simple to the extreme. Solomon Golumb tackled many different puzzles dealing with polyominoes, which he created in 1955 [4], shapes similar to dominoes but are not restricted to the rectangle formed by two halves that are well known. Figures will later be introduced which are constructed in a similar manner. To understand how the polyominoes are constructed we must be familiar with a few terms.

Definition 2. A *polyomino* is a polygon formed by one or more edge-connected squares constructed from a square lattice's cells; an entire cell of the square lattice acts as the primitive base.

Definition 3. Two polygons are *equivalent* if one can be rotated and/or reflected and/or scaled to

create two congruent polygons; distinct chirality does not make two polygons non-equivalent.

Definition 4. The *order* of a polyomino is determined by the number of bases utilized to form it.

Definition 5. Two polygons are *isometries* of one another if one may undergo a series of distance-preserving transformation between metric spaces.

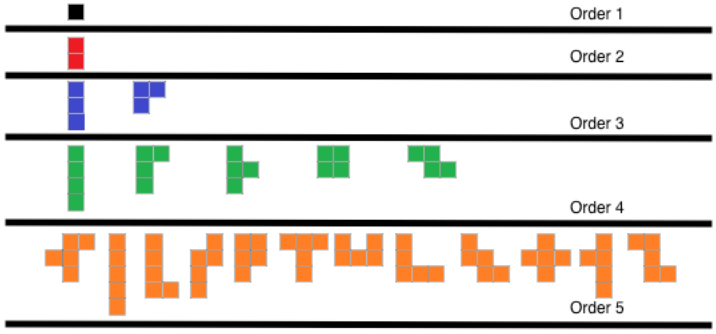

Figure 6: Polyominoes set examples

One may question "How we know the sets given in Figure 6 are complete?" For example, why aren't there more of order 2? One could rotate the red polyomino shown to create a horizontal version of this, but it is still far too similar to the original. The best known polyominoes are perhaps the tetrominoes [4] which are seen in the game of Tetris which utilizes polyominoes of order 4. One may argue that more polygons should be present in this set but these would be isometries or equivalencies of polyominoes that already exist within the list shown.

What sort of puzzles can be created with these tetrominoes? These five elements have a total area of 20 square units as each is made up of four squares. A natural question to ask is if it possible to form a 4×5 rectangle using these five tetrominoes as pieces? We can prove that this is impossible.

Take the 4×5 rectangle and checker the unit squares black and white so that each unit square is of an alternate color to those orthogonally adjacent. Do the same with the five different tetrominoes.

We see that four of the five pieces are *balanced*; each has the same number of black and white squares. The "T" however is imbalanced as it will have one white and three black or vice versa. The 4×5 rectangle has an equal number of squares of both colors; it is balanced with 10

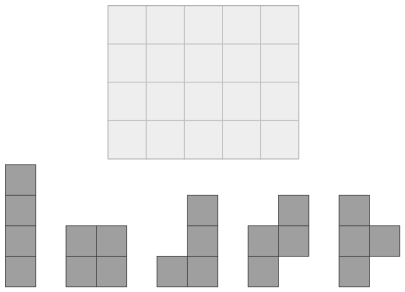

Figure 7: 4x5 Rectangle and Tetrominoes

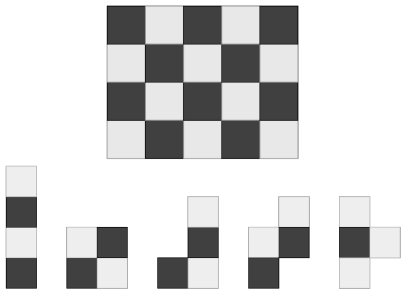

Figure 8: 4x5 Rectangle and Tetrominoes Checkered

white squares and 10 black squares. Due to the imbalance of our five pieces we will have either 8 white squares and 12 black squares, or 12 and 8 respectively. It is therefore impossible to lay the five pieces upon the 4×5 rectangle. This is often referred to as *parity-imbalance*.

An interesting observation comes up when we construct the next set of polyominoes, each new set an order larger than the last by 1. Looking at the number of unique polygons that may be constructed: when composed of a single base square there is 1 figure, with two squares again 1 figure, with three there are 2, then 5, 12, 35, 108, 369, and the list keeps growing. There is no specific formula for determining the quantity of polyominoes there will be of a specific order, but we are able to place bounds on the cardinality of a set of polyominoes of a given order utilizing *Klarner's Constant*, the limit growth rate of polyominoes λ for polyominoes of order n.

This value is discreetly discussed in the Barequet's paper [1]. Their paper also provides proof for providing an upper bound for the growth rate $\lambda \leq 4.5685$, which is at this point the most accurate upper bound for λ. The lower bound until recently was 3.98, but has recently been verified to be greater than 4.

With this knowledge in hand, it would give credit to the idea that the cardinality of sets utilizing any particular base, varying in order, will increase in a similar manner with some form of growth rate constant. Likely not the same, but the notion tells us that the set of any order n will always be finite in number.

Different sets of pieces have been created with the same method to that of polyominoes, but with a different base [10].

Definition 6. A *polyform* is an element of a set of polygons constructed by using a polygon as a base and joining copies under a set of given rules.

Definition 7. A *region* is a polygon with an area correlating to a specific set of polyforms.

Polyforms simpler to understand and recognize utilize regular polygons as their base (Figures 4(b) and 5(b)). Figure 9 shows examples of polyforms, varying in base and order, in recognizable configurations. Both a simple and more complex layout is provided [5]. The first pair utilizes pentominoes; a set of polyominoes of order 5. The second pair utilizes hexiamonds; a set of polyforms made using a lattice such as shown in figure 3(b) and creating a set of order 6. The last uses heptiamonds; similar to hexiamonds but of order 7. A comprehensive list of polyiamonds is made available through Goodger's work [5].

We take special note of these regions as they form a recognizable shape or pattern overall, but these examples are a drop within the plethora of regions that could be constructed using the three polyform sets mentioned.

Let P be a set of polyforms (such as the set of pentominoes or a subset of hexiamonds). Let R be a region on the plane. Let A be a function that takes in either P or R and give a real number to represent the area of all polyforms in the set P or the area enclosed within the region R. These are $A(P)$ and $A(R)$ respectively. When $A(P) = A(R)$, we look to see if we may exhaust P and lay each polyform within the region R such that there is no space left within R left uncovered. Such a layout(s), if it exists, is called a *solution*.

Triangles have the least number of sides and vertices possible for a polygon, it's impossible to create concave triangles, and we can take any polygon, be it regular or irregular, and show that

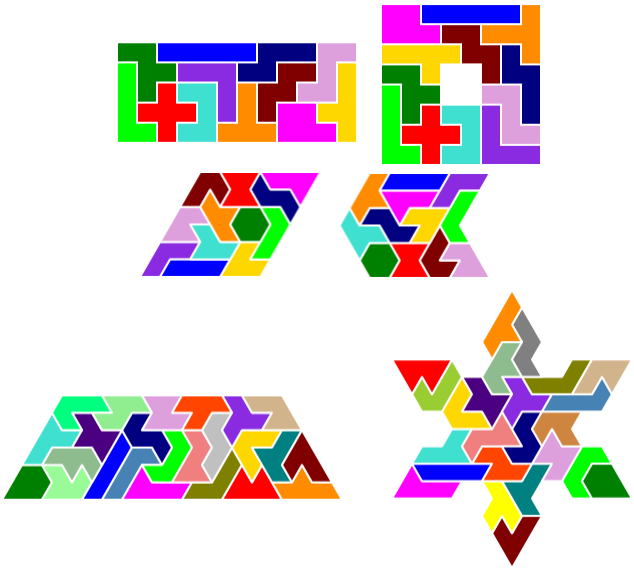

Figure 9: Polyform Layouts (featuring pentominoes, hexiamonds, and heptiamonds)

it may be compiled by some finite quantity of triangles. O' Rourke's work [9] utilizes computers to prove and expand upon this. Once done creating polyform sets using regular triangles (like the hexiamonds and heptiamonds), it's natural to consider a set based on a slightly more complex form; which brings us to the base shape for creating the set of polyforms this paper focuses on: the *drafter* which is a 30°-60°-90° triangle scaled to have an area of 1 unit.

In 1999, a Scottish enterprenour Christopher Monckton created a set of pieces using the drafter as a base. He offered a prize of one million pounds to anyone who could offer a solution to his challenge, the Eternity Puzzle, within four years of the puzzle's release. A regular dodecagon, shown in Figure 10 [2] was given for any to attempt to find a solution using provided pieces, a sub-set of dodecadrafters, which is the set of polyforms of order 12 that utilize the drafter as a base.

Only 209 of the set of 52630 possible dodecadrafters, no two being equivalent, were provided. Any dodecadrafters that that formed holes were excluded. Also, the pieces had no 30° vertices or "weakly hanging" triangles that could be easily broken apart upon handling. This was to ensure a "safer, sturdier" puzzle. A sturdy and weak example are shown in Figure 11 on the left and right respectively. A solution to the Eternity Puzzle is shown in Figure 12 [15]. The dodecadrafters that

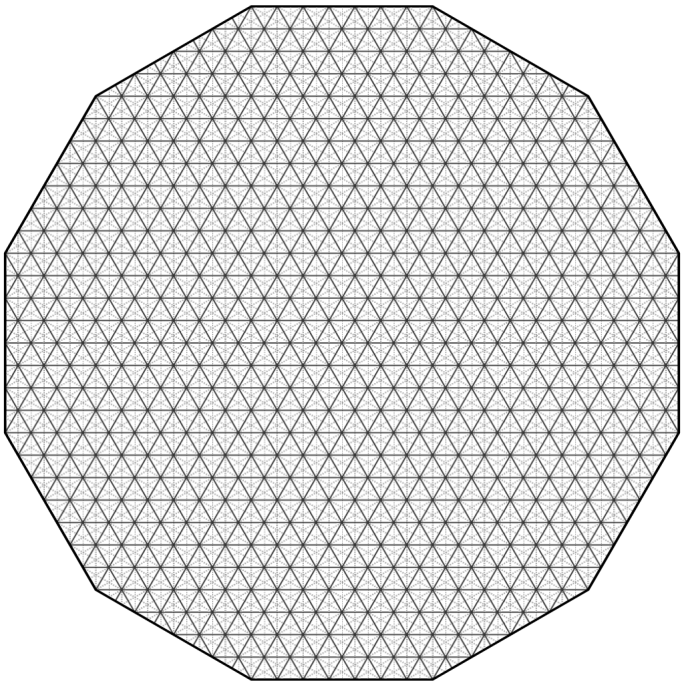

Figure 10: Eternity Region

were provided have specific (or lack of) properties.

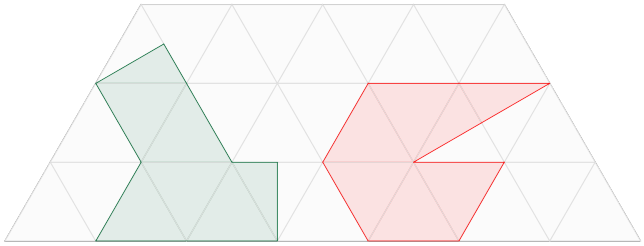

Figure 11: Sturdy and weak dodecadrafters

Half of prize money was put up by Christopher Monckton himself. The other half was provided by underwriters within London's insurance market. All solutions were to be mailed in and looked over on September 21 of 2000. If no solution was deemed correct, the following mailed in solutions would be looked over on September 30, 2001. This was to repeat until the year of 2003.

Christopher Monckton claimed that it would take three years or longer for any person(s) to

find a solution. He calculated that there were 10^{500} possible attempts at creating solutions. Given the puzzle's size, Monckton believed the puzzle "intractable" [14]

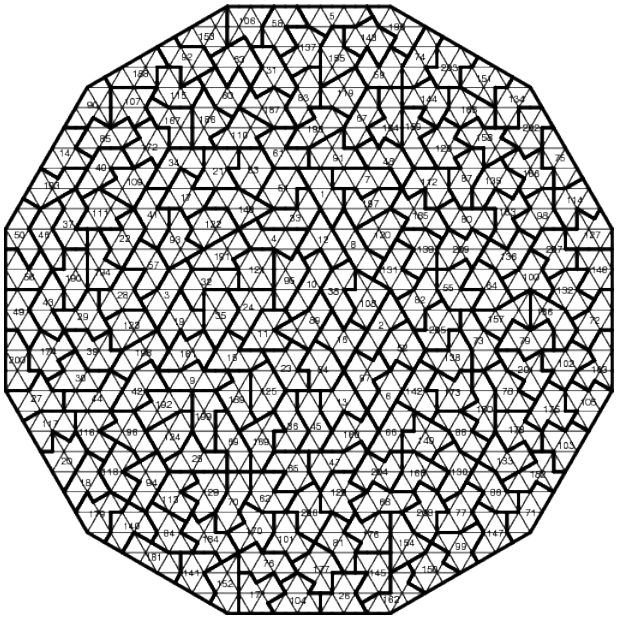

Figure 12: First public solution

The prize was claimed by Alex Selby and Oliver Riordan's a year later; their solution is shown in Figure 12. This solution was simply the first to be mailed in and accepted according to the rules given for said challenge. After the challenge had been completed, Cristopher Monckton apparently had to sell his home in order to pay this prize. Years later he made a statment that said his claim was a PR stunt meant to boost sales. Another solution was subsequently found by Guenter Stertenbrink [6], and there are many others. These solutions do not match clues that were given with the puzzle from Monckton describing his solution layout and Monckton never published his solution; this would imply that there are countless other solutions waiting to be discovered.

II. Drafters

Here, we introduce a simpler version of what was utilized in the eternity puzzle: polyforms of order 2 that use the drafter as a base.

Definition 8. A *polydrafter* is a polyform with a drafter used as a base and is constructed by joining drafters such that each is joined with at least one other by edges of non-zero length.

Definition 9. Given any polyform P, when possible to be placed such that each individual base rests entirely within a cell of the grid the base was made from, the polyform is *proper*. Otherwise, it is *improper*.

We will be focusing on the didrafters which are proper of which there are six. They are constructed and labeled as D_1 through D_6 in Figure 13.

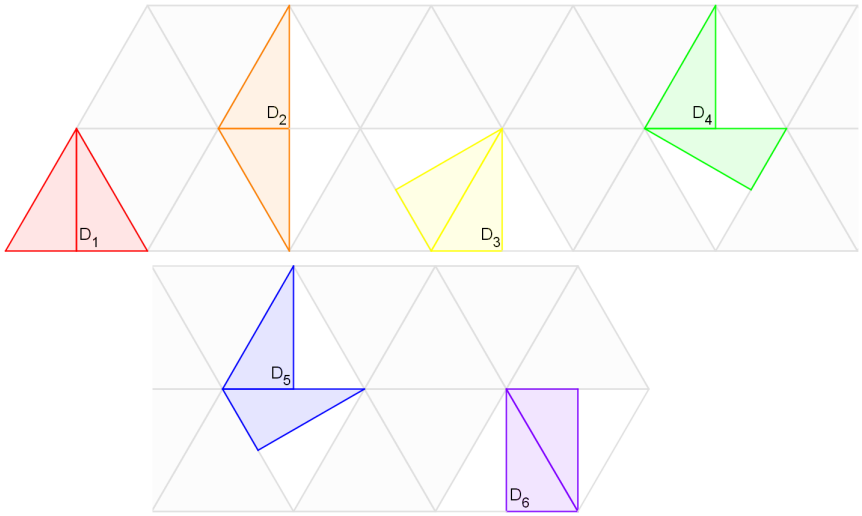

Figure 13: Proper didrafters

It's important to note that under the conditions laid out for creating polydrafters, they aren't necessarily proper. Examples of improper didrafters are shown in Figure 14. The quantity of improper didrafters is infinite. One could take any proper didrafters and translate one of the two drafters alongside the edge shared between the two any length.

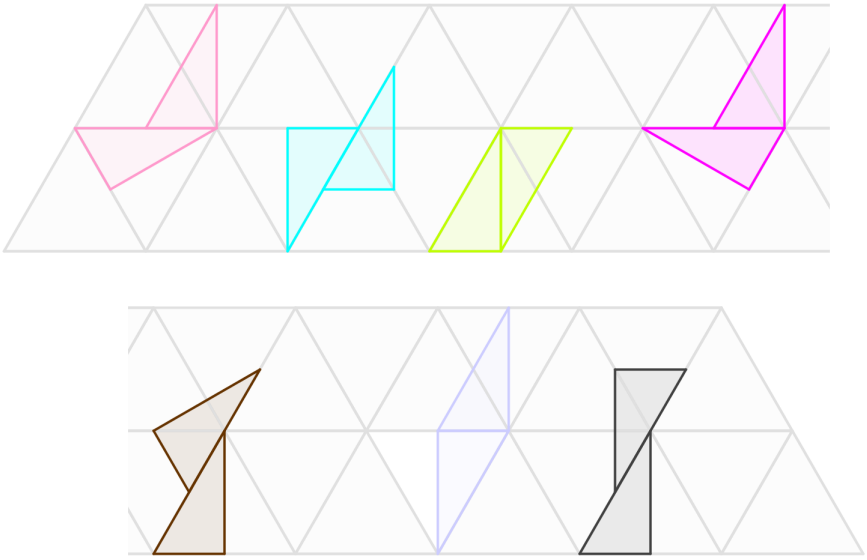

Figure 14: Improper didrafters

III. Tridrafters

III.1 Construction of the Tridrafters

From the didrafters (Figure 13) we construct *tridrafters* by adding a third drafter to any of the didrafters such that the new polyform is proper. This results in a polydrafter of order 3. An analysis of the tridrafters will be the main focus for the remainder of this thesis.

Figure 15 shows the complete set of tridrafters that may be constructed with this process. For example, T_1 through T_4 may each be constructed by adding a drafter to D_6.

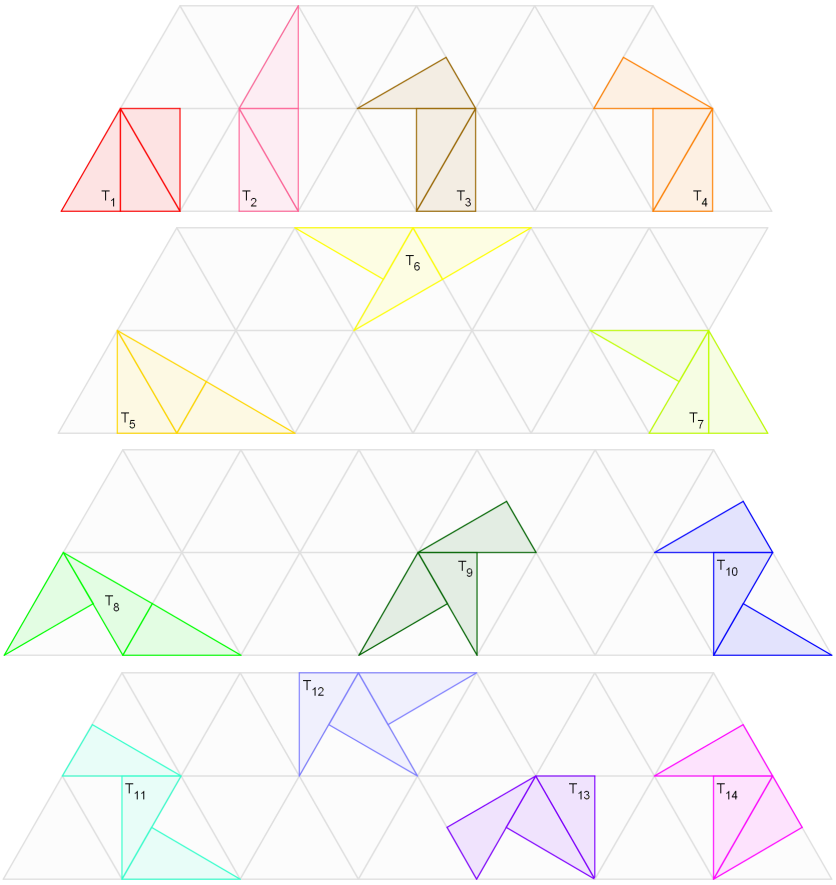

Figure 15: The Fourteen Proper Tridrafters (Coloring within the figure has no significance)

Let us scale the lattice such that the area of the cells is 2; this makes the area of a single drafter 1. Using 14 tridrafters, each having an area of 3, any polygon constructed by joining them together will have an area of 42. Any region R with an area of 42 may have a solution.

In Figure 16 below, there are regions with an area of 42 which may or may not have solutions. For simplicity, the regions chosen are convex and symmetrical.

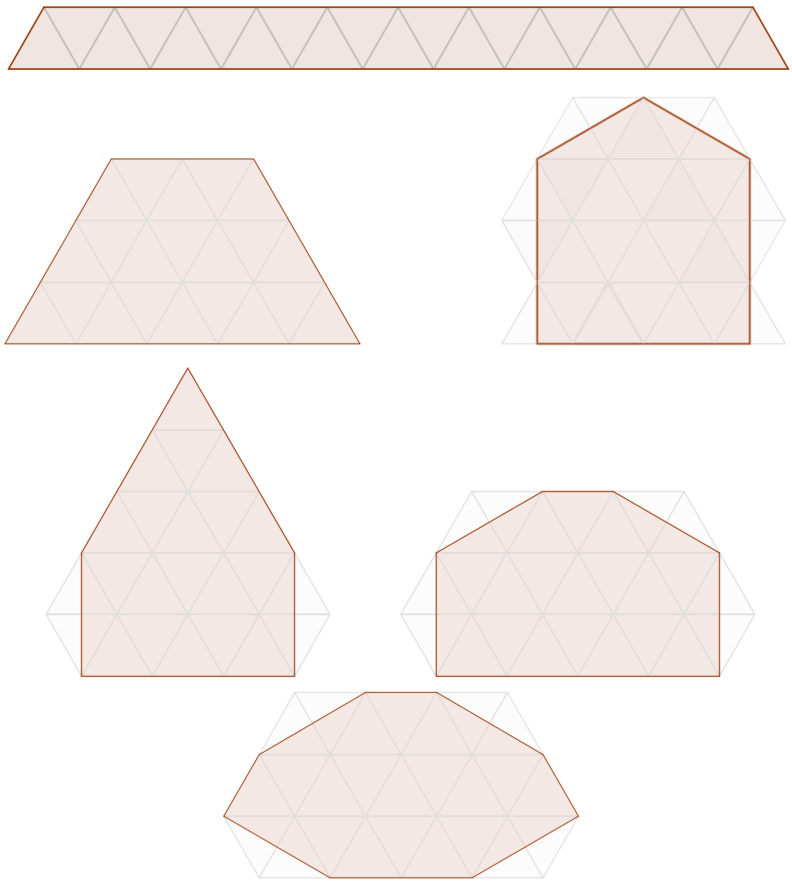

Figure 16: Sample regions

Though a region may have an area of 42 drafter units, this does not imply that a solution exists for it. The elongated trapezoid in Figure 16 for example. Bernd Karl Rennhak of Germany has made use of his own program and verified with the "Logelium Solver" that there are a total of 1516 possible convex regions with the needed area that can be considered. Additionally, only 75 of them have at least one solution, all of which may be viewed on Logelium's [12] website.

These numbers have been verified by other programs used to find solutions to puzzles in general, resulting in exhaustively finding all regions with every unique solution. The other trapezoid region, Figure 17, has two solutions and are simpler to observe than others as its edges conform to the edge set of the triangular lattice and will be the main reference for explaining properties found in all solutions.

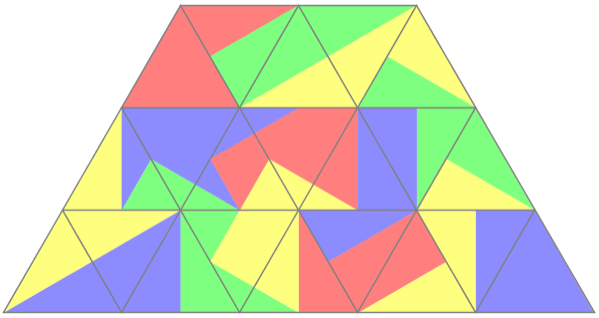

Figure 17: Trapezoid layout

III.2 Against-the-grain

The tridrafters that are utilized to form solutions for regions, defined as being proper, have the capability of being placed *with-the-grain*; a state of being placed in alignment with the lattice grid. While this is true for all the tridrafters individually, when two Tridrafters are connected they are not necessarily placed with-the-grain simultaneously. Figure 18 shows two tridrafters placed with-the-grain on the left and the same two tridrafters placed against-the-grain to the right.

In the figure below, we see the triangular lattice constructed utilizing the black nodes. Lines can be drawn through these black nodes to form the triangular lattice used to created the tridrafters. Each of the red nodes represents a midpoint between each pair of black nodes. When tridrafters are placed with-the-grain together such as the pair on the left, the vertices of the hypotenuse lie upon the black nodes forming an equilateral triangle between the drafters joining the tridrafters.

We describe placement as *against-the-grian* when this does not occur. When a tridrafter is placed against-the-grain but the vertices that make up the hypotenuse lies upon red midpoint nodes instead, it is placed *orthogonally against-the-grain*. Note how here a parallelogram is formed between the drafters joining the tridrafters.

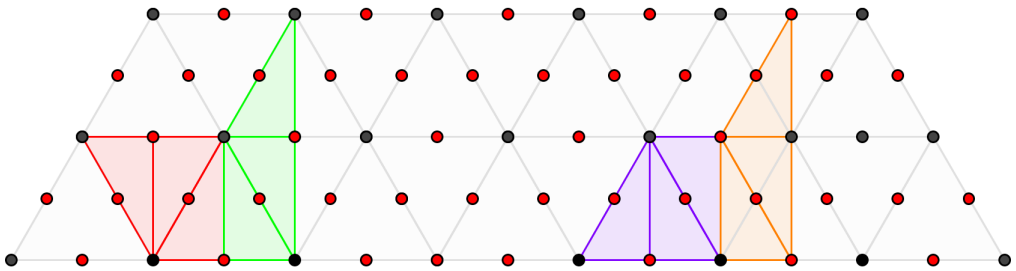

Figure 18: Tridrafters with and against-the-grain

A solution for a region is with-the-grain if and only if all tridrafters within the solution lie with-the-grain simultaneously. A solution for a region is against-the-grain otherwise.

Working with the trapezoidal region one is able to systematically look for solutions. During this process we find it increasingly difficult to keep tridrafters both with-the-grain and within our

region's border. In trying to do so we often come to a point where we are seemingly forced to cross the border or create a hole which is impossible to fill. This is known as a *breach* and a *void* respectively.

The trapezoid has four corners, two of which measure 60° and the other two 120°. These will act as our starting locations for the placement of tridrafters to look into how our potential solutions would need to be structured. The first corners to look at will be the 60° corners. We may use a single tridrafter that contains a 60° angle or two tridrafters that contain 30° angles to fill in a corner of this measurement.

Lemma 1. *Either both T_1 and T_7 are placed in the 60° corners of the trapezoid, or one of the two are used with the other corner being filled with T_2, T_5, or T_6; two of these three used in tandem with one another.*

Proof. There are two different methods to fill a 60° corner. Utilize a single tridrafter that contains a 60° angle or by connecting two 30° corners of two individual tridrafters.

Only T_1 and T_7 contain a 60° angle and can be placed in said corner with-the-grain. Of the tridrafters that contain 30° corners, only T_2, T_5, and T_6 (only one of its three angles) can be used without causing a breach or a forming a void. □

The 120° corners are larger and therefore have a wider spread of choices for how to fill them. We may use a single tridrafter that contains a 120° angle, use two tridrafters that contain a 90° angle and 30° angle between them, use two tridrafters that contain two 60° angles between them, use three tridrafters that contain a 60° and two 30° angles between them, or use four tridrafters that contain four 30° angles between them.

Corollary 1.1. *It is impossible to fill a 120° corner utilizing only tridrafters with 60° angles as only T_1 and T_7 have the necessary 60° angles to be joined to fill in said corner and at least one must be placed to fill a 60° corner.*

Lemma 2. *Only T_1 or T_7 exclusively may be used to fill in a 120° corner.*

Proof. T_1 and T_7 are the only tridrafters that contain a 120°. If either of these are utilized to fill in a 120° corner, the other must imediately be utilized for one of the two 60° corners as shown in Lemma 1 making it impossible to use both for 120° corners. □

Lemma 3. *To fill in corner larger than* 60° *utilzing a* 90° *angle, the* 90° *angle must be formed by two individual drafters.*

Proof. The 90° angles may be formed by either individual drafters or two joined drafters. The former with the altitude and base of the drafter acting as edges of the overall tridrafter. The latter with the 60° and 30° angle being joined. Should the single drafter be used, it will always lie against-the-grain. Thus we are forced to utilize tridrafters with 90° angles formed by two individual drafters. □

Lemma 4. *It is impossible to have a with-the-grain solution utilizing two tridrafters connecting a* 90° *and* 30° *degree angles to fill in the* 120° *corner of the trapezoidal region.*

Proof. From Lemma 3, only T_1, T_2, and T_8 may be utilized for their 90° angles.

When T_1 is placed in one of the 120° such that its 90° angle is covering part of the corner, of the remaining tridrafters to connect to it to fill this corner: If T_2 is utilized, only T_7 or T_8 may be attached T_2's right angle. Using the former would violate Lemma 1. When using the latter, only T_5 and T_6 can be attached to T_8. In connecting tridrafters to T_8, choices that don't cause breaches or voids will cause a hole in the shape of T_1 to form. As this is already being utilized, we cannot fill said hole. If T_5 is utilized, due to Lemma 1, T_2 and T_6 along with T_7 are placed in the 60° corners. At this point, no tridrafters can be joined to T_5 without causing breaches or voids. If T_6 is utilized, due to Lemma 1, T_2 and T_5 along with T_7 are placed in the 60° corners. At this point, no tridrafters can be joined to T_5 without causing breaches or voids. If T_7 is utilized, we breach Lemma 1. If T_8 is utilized, a 120° angle is formed; it will not be possible to fill this. If T_9 is utilized, only T_7 or T_8 can connect to it. When using T_7, we breach Lemma 1. When using T_8, T_2 and T_6 can connect to it. When using T_2, T_5 and T_6 must be used with one another to connect to T_2 and T_7 will go in the other 60° to follow through with Lemma 1. Nothing remains to connect to T_7 without causing breaches. When using T_6, T_2 and T_5 must be used with one another to connect to T_6 and T_7 will go in the other 60° to follow through with Lemma 1. Nothing remains to connect to T_7 without causing breaches. If T_12 is utilized, only T_2 can be connected to it. T_5 and T_6 along with T_7 must fill the 60° corners to adhere to Lemma 1; nothing may connect to T_2

without causing a breach or a void.

When T_2 is placed in one of the 120° corners such that its 90° angle is covering part of the corner, of the remaining tridrafters to connect to it to fill this corner: Only T_5 may be connected to fill this corner. Nothing can connect to T_5 without causing breaches or voids.

When T_8 is placed in one of the 120° such that its 90° angle is covering part of the corner, of the remaining tridrafters to connect to it to fill this corner: If T_2 is utilized, only T_7 can connect to it. At this point, T_5, T_6, and T_1 must be placed in the 60° corners. If T_5 and T_6 are placed in the 60° on the same side as T_8, T_1 must be placed on the other. Nothing can connect to T_1. If T_1 is placed in the 60° on the same side as T_8, T_5 and T_6 must be placed on the other. T_5 and T_6 may be oriented in two different ways; either will result in nothing but breaches or voids when other tridrafters are joined to them.

It is therefore impossible to have a with-the-grain solution utilizing two tridrafters to form a 120° angle using a 90° and 30° angle between them. □

Lemma 5. *It is impossible to fill a* 120° *corner using four* 30° *angles from four tridrafters and have a with-the-grain solution.*

Proof. There are very few unions of Tridrafters that create 120° angles from four 30° angles. One is shown in Figure 19; these four tridrafters (T_2, T_5, T_6, and T_8) only work due to their elongated nature allowing for us to maneuver the pieces around.

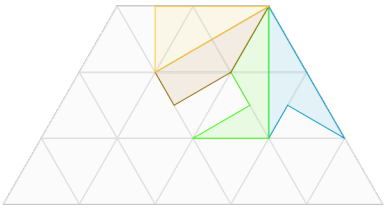

Figure 19: Four 30° angles forming a 120° angle

Using other tridrafters with 30° angles forms voids or breaches prohibiting us from using any other than these four. T_2, T_5, or T_6 must be utilized for the 60° corners by Lemma 1. As we need all four of these tridrafters to create the 120° corner and as at least one will be made

unavailable, we cannot fill in a 120° corner in this way. □

Lemma 6. *It is impossible to utilize both T_1 and T_7 to cover both 60° corners of the region and have a with-the-grain solution.*

Proof. Assume that both T_1 and T_7 are utilized for their 60° angles to fill the two 60° corners. This will leave the 120° angles to be filled by other means. From Corollary 1.1, Lemma 4, and Lemma 5, we may conclude that only utilizing three tridrafters, one with a 60° angle and the other two with 30° angles are available. Only T_5, T_{13}, and T_{14} have 60° angles and are available. When T_5 is placed so that its 60° angle is placed within the 120° corner such that it lays with-the-grain, it may be oriented in one of two ways. In either, only T_2, T_6, or T_8 may connect to it specifically alongside T_5's longest edge. If T_2 is utilized, only T_8 may join to it. Doing this causes a 120° corner to form; there are no combinations of tridrafters available to fill in this newly formed corner. When T_{13} is placed so that its 60° angle is placed within the 120° corner such that it lays with-the-grain, a void is formed. When T_{14} is placed so that its 60° angle is placed within the 120° corner such that it lays with-the-grain, a void is formed.

It is therefore impossible to utilize both T_1 and T_7 for both 60° corners of the region. □

This allows us to replace Lemma 1 with the following as follows:

Lemma 7. *Either T_1 or T_7 exclusively is placed in the 60° corner of the trapezoid with the other corner being filled with T_2, T_5, or T_6; two of these three used in tandem with one another.*

Lemma 8. *Either T_1 or T_7's 120° corners must be utilized to fill one of the 120° corners of the region to create a with-the-grain solution.*

Proof. From Lemma 4, Lemma 5, and Corollary 1.1 we can conclude that the only ways to fill the 120° corners is with T_1 or T_7's 120° angle and a combination of one 60° angle with two 30° angles, or two combinations of the latter.

The only tridrafters that contain 60° angles are T_1, T_5, T_7, T_{13}, and T_{14}. When either T_{13} or T_{14} is placed in one of the 120° corners such that it's 60° angle covers part of the 120° corner and lays with-the-grain, it will cause a void. When either T_1 or T_5 is placed in one of the 120°

corners such that it's 60° angle covers part of the 120° corner and lays with-the-grain, the other is immediately reserved for one of the 60° corners by Lemma 7 and T_5 must be placed in the other 120° corner. When T_5 is placed in one of the 120° corners such that it's 60° angle covers part of the 120° corner and lays with-the-grain, it may be placed in one of two orientations. With both, only T_2, T_6, and T_8 may connect to it alongside its longest edge. If T_2 is utilized we violate Lemma 7. If T_6 is utilized we violate Lemma 7. If T_8 is utilized we cause a void. Therefore T_5 cannot be utilized to fill in a 120° corner. Thus there are not enough eligible 60° angles to be used with this method to cover both 120° corners. □

Corollary 8.1. *It is impossible to create a with-the-grain solution utilizing a* 60° *angle with two* 30° *angles between three tridrafters filling a* 120° *corner.*

Through the use of these lemmas, we are able to conclude the following theorem.

Theorem 9. *It is impossible to have a with-the-grain solution for the trapezoidal region.*

Proof. By Lemma 4, it's impossible to fill either 120° corner by using two tridrafters, one with a 30° angle and the other with a 90° angle. By Lemma 5, it's impossible to fill a 120° corner using four tridrafters with 30° angles. By Corollary 8.1, it's impossible to fill a 120° corner using a 60° angle with two 30° angles between three tridrafters. We may then use only T_1 and T_7 to fill in either 120° corner. In doing so, by Lemma 7, the use of one will remove the possibility of using the other for the second corner. At this point, we have no valid options to fill in the second 120° corner. □

As there is no with-the-grain solution for the trapezoid due to the interaction between the tridrafters often being forced to cause breaches or voids, a natural query would be if it's just as difficult to create a with-the-grain solution for any convex region.

Conjecture 1. *Every solution to a convex region will have tridrafters placed against-the-grain.*

This is what we wish to prove due to the lack of any counter-proof to this claim from any discovered solutions to any region.

Figure 20 shows a solution for the trapezoidal region in tandem with a drafter grid that aligns with the tridrafters respectively laid upon the region. Looking at this, we can see that the

trapezoid region is composed of 21 full cells or 42 drafter units. At first glance, the tridrafters as placed in the given solution, may appear to be with-the-grain. Looking closer though, one can observe that there is a section of four tridrafters that exhibit the against-the-grain trait. These 4 pieces are with-the-grain in relation to one another as shown in Figure 20 in gold. The other 10 tridrafters are with-the-grain in relation with one another as well shown in green. This solution has two different underlaying drafter grids, the one in gold and the one in green.

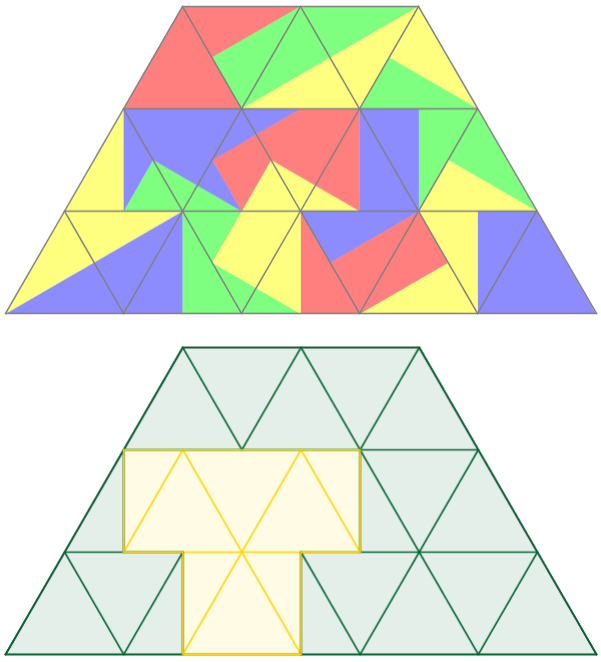

Figure 20: The "T" Section

There is only one other known solution to the trapezoid region crafted by removing the four tridrafters in the gold area that make up the "T" section out, performing an action of vertical reflection on all four tridrafters, and placing them back in the same "T" section which will have no effect upon the gold and green drafter grids drawn in Figure 20. Looking at these two colored drafter grids we see that the smaller gold portion is similar to the green drafter grid. It's as if the original grid shifted horizontally so that what would be black nodes in Figure 18 were now at red nodes. It seems that if we're to find a solution we'll have a sub-region that does not rest upon the same drafter grid that the majority of the tridrafters in the solution do.

A solution for two different convex shapes are shown displaying this same feature in Figure 21. The green and yellow grids that lay beneath the solutions illustrate the against-the-grain grid shift between the two sub-regions. The right configuration shows that regions with the same underlying grid can be entirely disjointed from one another similar to the trapezoid region's solutions.

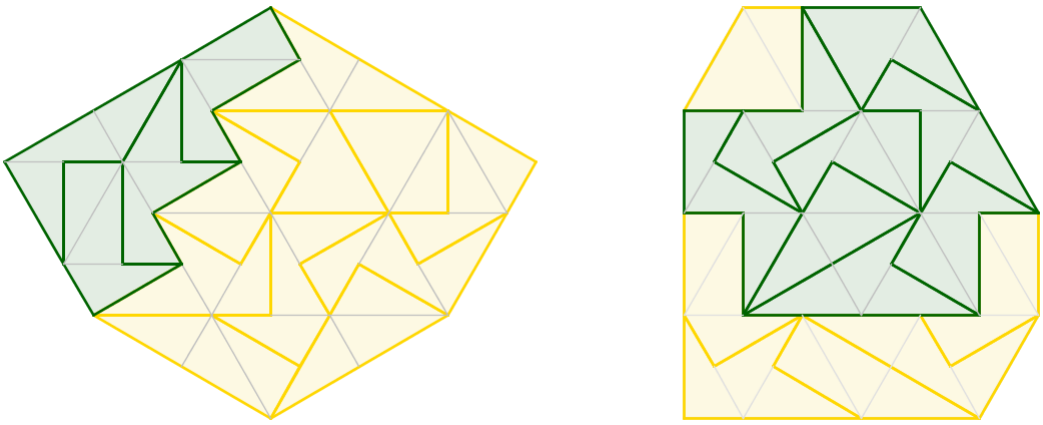

Figure 21: Other convex tridrafter layouts

This characteristic is identified most easily with what was shown in Figure 18 Tridrafters are placed orthogonally against-the-grain and form parallelograms similar to the third improper didrafter depicted in Figure 14 rather than equilateral triangles when joined.

Another natural question that may arise is "Why is this characteristic so common?" There are facts about this set of 14 tridrafters that give credence to the idea of the against-the-grain property of being common, if not necessary. Let's first assume that a person is attempting to create solution that is with-the-grain.

Definition 10. A polydrafter has *acute valence* if it has at least one concave angle present.

The degree of acute valence will vary depending on how many concave angles are present. $T_{1/2/5}$ have an openness of degree 0, $T_{3/4/6/7/8/13/14}$ of 1, and $T_{9/10/11/12}$ of 2.

Let P be a polygon constructed of joined tridrafters that is concave due to an arbitrary angle θ. Let T be a tridrafter or union of linked tridrafters separate from P. If T can be placed and

linked to P such that the resulting polygon is convex, we say that T has *completed* θ.

Definition 11. A polygon has *convex completion* if there is no internal angle θ which has a value greater than 180 degrees.

Theorem 10. *To create a convex polygon when linking Tridrafters, altitudes must be linked to close it.*

Proof. Assume two tridrafters T_m and T_n are linked together. Assume one of the tridrafters, T_n has an open 270° angle. The 270° degree angle must be closed for the resultant polygon to be convex. This can only be done by linking tridrafter T_m with a 90° corner to the 270° corner of tridrafter T_n. 90° angles are present only with the right angle of a single drafter, formed by the altitude and base acting as the rays of the angle, or the joining of a 60° and 30° angle between two drafters, formed by the altitude and hypotenuse acting as the rays of the angle of said two drafters. If we utilize the former to close, either the base or altitude of T_m must link to the altitude of T_n. If the base is used to link the two, the result will not be convex. If the altitudes are linked, the result may be convex. If we utilize the latter to close, either the hypotenuse or altitude of T_m must link to the altitude of T_n. If the hypotenuse is used to link the two, the result will not be convex. If the altitudes are linked, the result may be convex. Thus, tridrafters must be linked by altitudes to create a resultant convex polygon. □

Theorem 11. *To create a convex polygon with-the-grain, the* 270° *angle must be closed utilizing a right angle formed by a single drafter. (This will be referred to as an aligned angle).*

Proof. Assume tridrafter T_n is open. Assume two tridrafters T_m is closing T_n. Assume the two tridrafters T_m and T_n lie with-the-grain in relation to one another. Based on the first theorem we must use the altitude from a right angle formed from a single drafter or the right angle formed by two drafters. If we link altitudes of right angles formed in the latter format, an against-the-grain shift between the two is created contradicting our assumption. Thus we can only close a 270° angle utilizing aligned angles. □

Figure 22 depicts all tridrafters and labels the reflex and aligned angles.

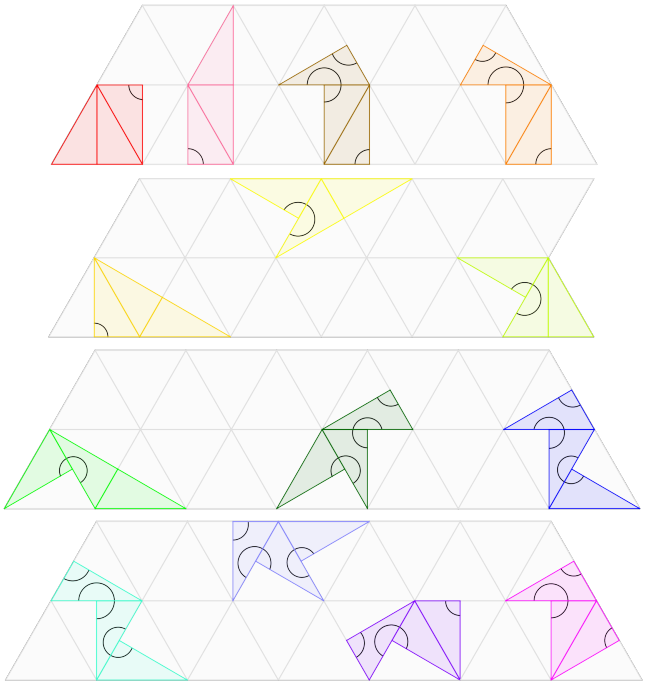

Figure 22: The Aligned and Reflex Angles within Tridrafters

Theorem 12. *All aligned angles must close a* 270° *open angle.*

Proof. Assume all tridrafters are aligned with-the-grain Assume the tridrafters all fit within a convex region with an area of 21 cells There are a total of fifteen 270 degree internal angles between the 14 tridrafters. There are a total of fifteen aligned angles. Each of the fifteen 270 degree internal angles must be closed to prevent the resultant polygon from being concave. Thus, to create a convex with-the-grain configuration, there must a 1:1 utilization between each 270° and 90° angle. □

Looking at these theorems, it's would seem prudent to observe what type of layout emerges when we close one tridrafter with a second. The goal is to create a fully closed polygon so we'll take a look into if, when closed, the degree of openness is reduced, remains constant, or increases. In the graph below, Figure 23, shows what occurs when each tridrafter is used to close tridrafter T_3.

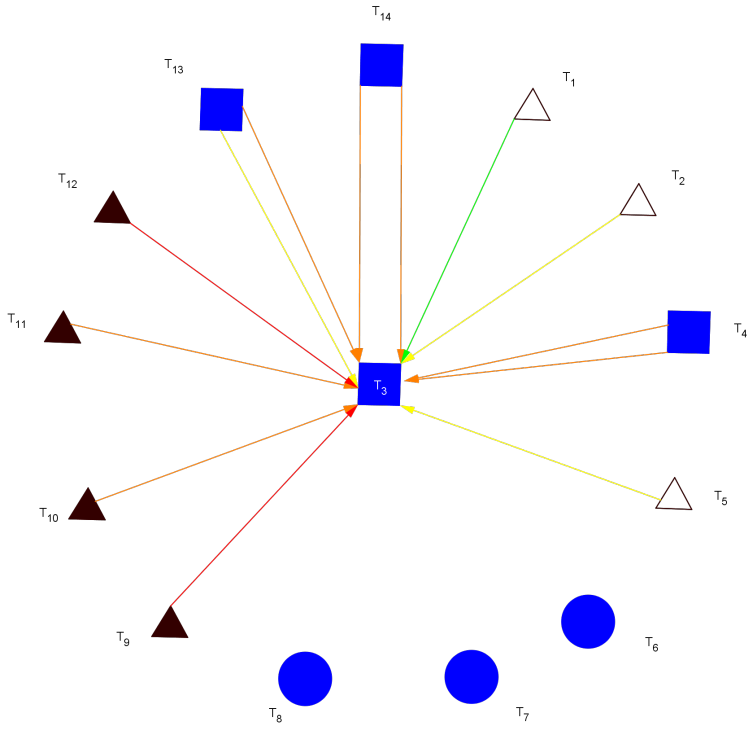

Figure 23: Closing T_3

The shape of each node shows how many available right angles the tridrafter has, or how many options there are to close an open tridrafter. Circles have zero available right angles, triangles have one, and squares have two. The coloring of said nodes represents the degree of openness of the tridrafter. Uncolored nodes have a degree of 0, blue nodes of 1, and black nodes of 2. Lastly, the color of the arcs joining the 13 tails to the featured head, the tridrafter in the center, represents how the degree of openness changes upon closing. Green represents that no new concave angles are formed causing the degree of openness to fall by 1, yellow represents that one concave angle is formed keeping the degree constant, orange represents that two concave angles are formed increasing the degree by 1, and red represents that three concave angles are formed causing the degree to increase by 2.

All graphs of this nature can be found in VIII.1 in the appendix section.

Due to the nature of the tridrafter, verified by the graphs shown, we can observe a few properties of the relation attaching tridrafters together has. The circular nodes will never be on the

tail end of an arc as they have no available right angles to close an open angle. Triangular nodes will act as a tail for one arc per right angle present in the tridrafter being closed. Square nodes will act as a tail for two arcs per right angle present in the tridrafter being closed. Uncolored nodes will never be on the head end of an arc as they have no open angles that need to be filled.

Looking at each of these 14 graphs, we see that only T_1 and T_2 have the capability of closing another tridrafter and reduce the degree of openness. This at least lends a strong argument for the idea that when attaching tridrafters together with-the-grain, a concave shape will result as all other tridrafters have new concave angles formed.

IV. Analysis of the Fourteen Tridrafters

IV.1 A Parity Analysis of the Tridrafters

According to the results of Rennhak's program, and assuming it's complete [12], we know of every solution to every possible convex region. We know then that it's impossible to create a convex solution with every tridrafter to be with-the-grain simultaneously. Hence our conjecture is true, but there is no underlaying mathematical reason to explain this. How does one go about trying to prove why a with-the-grain convex solution is impossible? The first thing done here is creating a method to mathematically quantify the pieces of the puzzle. We do this in two different ways. The first method uses the idea parity mentioned earlier. We create parity patterns by shading cells upon planes which are created in similar matter to those found and described in Levine's paper [7] on Plane Symmetry Groups. We're ensured the plane will repeat itself infinitely as it's generated in a manner conforming to the ideas established from Schattschneider's work [13].

Take an equilateral triangle on the plane with edge lengths of 2. Make one edge rest upon the x-axis and one vertex the origin point. Suppose all points of the triangle are rotated by $\frac{\pi}{3}/60^\circ$ about either endpoint to form a new triangle. Repeat this six times to form a hexagonal cluster of six cells. Color the upwards oriented cells black and the downwards oriented cells white. Suppose that every point on the plane is translated to the right by 6 with $T_1(\vec{x}) = \vec{x} + (6, 0)$ and translated diagonally up and right by $T_2(\vec{x}) = \vec{x} + (3, \sqrt{3})$. Repeating this action creates an infinite plane with a pattern that will be referred to as the *Up-Down* parity, Figure 24, with relative size for our use.

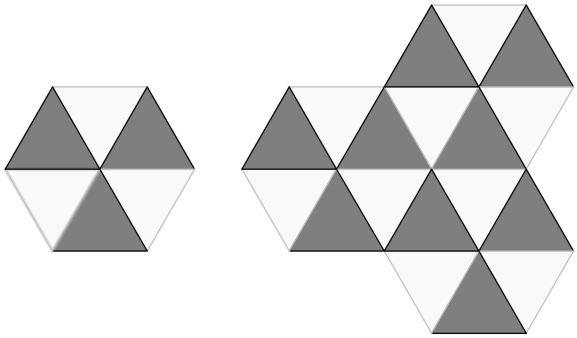

Figure 24: Up-down parity

Take the same triangular lattice to form the same hexagonal cluster of cells. Draw six altitudes, one for each triangle, starting from the vertex that is the center of the hexagonal cluster. This will create 12 half cells, drafters, and we will color the drafters black and white alternatively. Suppose that every point on the plane is translated to the right by 6 with $T_1(\vec{x}) = \vec{x} + (6, 0)$ and translated diagonally up and right by $T_2(\vec{x}) = \vec{x} + (3, \sqrt{3})$. Repeating this action creates an infinite plane with a pattern that will be referred to as the *Left-Right* parity, Figure 25, with relative size for our use.

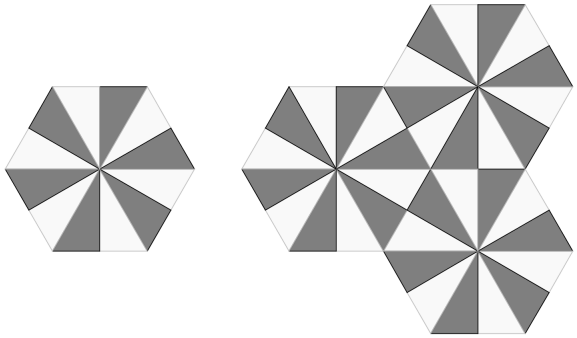

Figure 25: Left-Right parity

Take the same triangular lattice to form the same hexagonal cluster of cells. Draw six altitudes, one for each triangle, starting from the vertex that is the center of the hexagonal cluster. This will create 12 half cells. Within one of these six cells we will color 1 of the halves black and the other white. The cell to the right in a clockwise fashion, we'll color the first half white and

then the second black. We will continue this pattern for all six cells. Suppose that every point on the plane is translated to the right by 6 with $T_1(\vec{x}) = \vec{x} + (6, 0)$ and translated diagonally up and right by $T_2(\vec{x}) = \vec{x} + (3, \sqrt{3})$. Repeating this action creates an infinite plane with a pattern that will be referred to as the *East-West* parity, Figure 26, with relative size for our use.

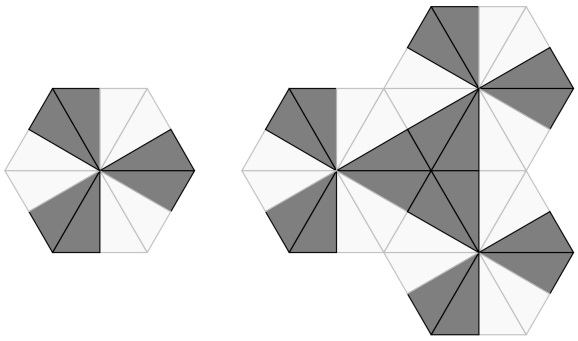

Figure 26: East-west parity

The following figure, Figure 27, divides the hexagonal area into 12 half-cells. Giving value to these half-cells, 1 to the shaded and -1 to the unshaded, allows us to assign value that can describe the tridrafters relative to the various orientations they may be placed in.

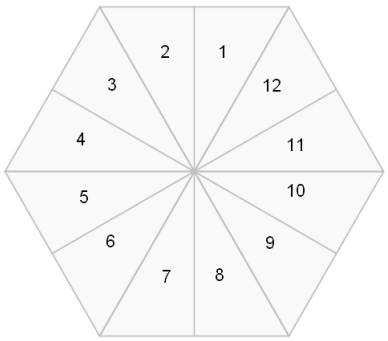

Figure 27: Numbering of the different orientations of the half-cell

We follow this process to give a value to the polydrafter.

1. Place the polydrafter, composed of n drafters, with-the-grain upon the triangular grid shaded with the up-down parity.

2. Separate the polydrafter into the n number of drafters that compose it while maintaining the individual drafter's orientation.
3. Place each drafter upon the single one of the twelve orientations the piece will fit into.
4. Give the value of 1 to the drafter if placed in a shaded half-cell or a value of -1 if placed into an unshaded half-cell.
5. Add the n number of values together; this sum will be referred to as a.
6. Repeat process with the left-right parity to obtain b; repeat process with the east-west parity to obtain c.

We use these three parities which were created by Ed Pegg Jr. [11], not necessarily created from the above explanations, they are just processes of recreating said patterns.

If we apply these patterns to our lattice and place our drafters upon the grid, then we are able to give three values to each drafter and therefore tri-drafter, one from each parity. When we place a drafter onto the grid for one method, it stays in that same orientation for the other methods; only the grid pattern behind it is changed to give the other needed values.

It is important to keep in mind that we are *not* placing the entire tridrafter into the grid as one piece. We are looking at the orientation of each individual drafter that composes the polydrafter, measuring each of their values, and then adding all values together. An example with T_1 is given in Figure 28. We see a drafter with an orientation of 2, 7, and 8. These three drafters have parity measurements of $\langle -1, -1, 1\rangle$, $\langle 1, 1, 1\rangle$, and $\langle 1, -1, -1\rangle$ respectively. Adding these three values together gives T_1 the values $a = 1$, $b = -1$, and $c = 1$ with respect to its current placement.

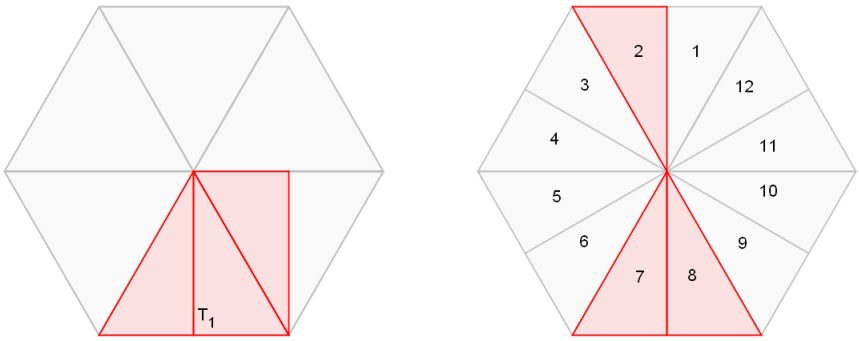

Figure 28: T_1's drafter orientations

Definition 12. Let R be a figure (polydrafter, region, etc.). We define p as the function that takes R and maps it to the 3-dimensional vector $\langle a, b, c \rangle$ where a, b, and c are the parity values as defined in the measuring process. We call $\langle a, b, c \rangle$ the *parity vector* of R.

As a tridrafter can be placed into the grid in a multitude of ways there are multiple parity vectors associated with each tridrafter. This vector will alter whenever the tridrafter is rotated 60° represented by the action σ, or reflected represented by the action τ. Ultimately, any single tridrafter may have one of four parity vectors, very similar in composition, dependent on its orientation.

Figure 29 shows the effects of rotational and reflective transformations.

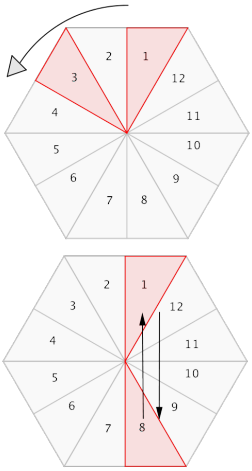

Figure 29: T_1's Orientations Rotated and Reflected

Theorem 13. *Given a polydrafter T with $p(T) = \langle a, b, c \rangle$, $p(\sigma(T)) = \langle -a, b, -c \rangle$.*

Proof. Any polydrafter may be measured through the process described relative to Figure 28. If the polydrafter is rotated 60° then all drafters composing the polydrafter rotate 60°. The Left-Right parity has rotational symmetry in increments of 60° resulting in the Left-Right value being unaffected when the drafter is rotated 60°. The Up-Down and East-West Parities have rotational symmetry in increments of 120° with the half-cells altering between shaded and unshaded every 60°. Therefore any drafters rotated 60° will not have its Left-Right value altered; the Up-Down measurement and East-West measurements are negated. □

Theorem 14. *Given a polydrafter T with $p(T) = \langle a, b, c \rangle$, $p(\tau(T)) = \langle -a, -b, c \rangle$.*

Proof. Any polydrafter may be measured through the process described relative to Figure 28. If the polydrafter is reflected vertically then all drafters composing the polydrafter are reflected. The East-West parity has reflective symmetry resulting in the East-West value being unaffected when the drafter is reflected. The Up-Down and Left-Right Parities alter between shaded and unshaded with every reflection. Therefore any drafters reflected will not have its East-West measurement altered; the Up-Down measurement and Left-Right measurements are negated. □

Lemma 15. *Given a polydrafter T with $p(T) = \langle a, b, c \rangle$, $p(\sigma(\tau(T))) = \langle -a, b, -c \rangle$ and $p(\tau(\sigma(T))) = \langle -a, b, -c \rangle$*

Rotating and reflecting any polydrafter vertically will alter the parity vector's measurement from $\langle a, b, c \rangle$ to $\langle a, -b, -c \rangle$.

Proof. Rotating and reflecting the polydrafter one time apiece will cause the Up-Down parity value to remain unaffected due to being negated twice, and both values for the Left-Right parity and East-West parity will be negated. □

Corollary 15.1. *The parity vector of any polydrafter can only be altered to one of four forms: its original $\langle a, b, c \rangle$, as $\langle -a, b, -c \rangle$, as $\langle -a, -b, c \rangle$, or as $\langle a, -b, -c \rangle$.*

We can give a parity vector to a region as we do with polydrafters. We need only take the parity vectors of each orientation that is being covered within the region.

Table 1: Parities by position

Orientation	a	b	c
1	-1	1	-1
2	-1	-1	1
3	1	1	1
4	1	-1	-1
5	-1	1	-1
6	-1	-1	1
7	1	1	1
8	1	-1	-1
9	-1	1	-1
10	-1	-1	1
11	1	1	1
12	1	-1	-1

Note that a full upward cell may be covered by a pair of drafters in orientation 3 and 4, 7 and 8, or 11 and 12. Each of these pairs when added together give the resultant parity vector $\langle 2, 0, 0 \rangle$. A full downward cell may be covered by a pair of drafters in orientation 1 and 2, 5 and 6, or 9 and 10. Each of these pairs when added together give the resultant parity vector $\langle -2, 0, 0 \rangle$.

Lemma 16. *A region has the potential for a solution where all polydrafters are with-the-grain if and only if the region's border lays only upon the borders or upon the altitudes of the grid's cells.*

Proof. If we only connect the polydrafters with-the-grain then the border of the region the polydrafters create will lay upon the the grid's cell borders or altitudes. If the region itself has part of its border lying upon the cell borders or altitudes but other parts that do not, then the polydrafters can't be connected with-the-grain to form said region. □

What this tells us, is that out of the 75 convex regions that do have solutions, we need only to analyze the regions whose borders may allow for connecting tridrafters in a with-the-grain fashion. If a region already shows the signs of against-the-grain shifting, it doesn't have a solution where all of the tridrafters are connected as such. The trapezoid shown earlier, having its border lay only on cell borders, seemingly has the potential for a solution where all tridrafters are connected with-the-grain. This is because the region can be divided into properly placed drafters that can be associated with orientations as shown in Figure 30. We call regions like this *calculable*.

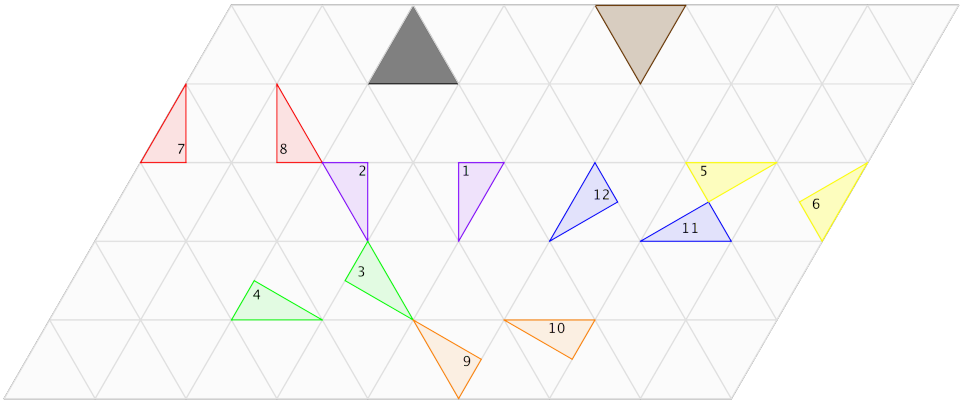

Figure 30: Coloring Orientations

In Figure 31, we see the parallelogram region. We see its upper, lower, and left edges laying upon the cell borders; the right edge however does not. No matter how one may shift this region on the grid, at least one edge will not lay on the borders or altitudes of cells simultaneously with all others. Regions like this *non-calculable*.

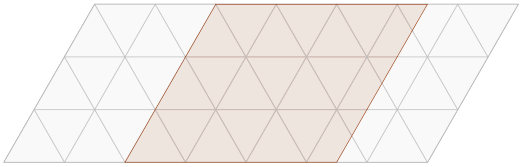

Figure 31: Parallelogram Region

Theorem 17. *If there is no combination of parity vectors that add up to a region's parity measurement then there is no proper solution.*

Proof. Assume there is a proper solution for a given region. If it exists then we would be able to measure the parity vector of each polydrafter within the region. Adding each drafter's parity vector would then result in the same parity vector of the region itself. If we can't find a combination that creates the desired parity vector, then no proper solution exists for the region. □

Regions which are non-calculable have no parity vector defined for them. This allows for the following lemma.

Lemma 18. *A non-calculable region will have no with-the-grain solution.*

If we perform a parity measurement upon the trapezoidal region in Figure 32, shown below, it has a parity vector of $\langle\ 6, 0, 0\ \rangle$. Looking through all combinations of manipulating our 14 tridrafter's parity vectors, there are some which do create a result of $\langle\ 6, 0, 0\ \rangle$. This doesn't mean that there are solutions that are properly connected; it simply doesn't rule out the possibility. (the method to find these combinations are explained in a later section) Theoretically, we may create more parities using similar processes that created the three used here. Often though the values will change with the same pattern showing no new relationships when rotating and/or reflecting, or the values have no recognizable cyclic pattern. These new parities are then often redundant or too complex to be of inherent use.

Figure 32 shows the trapezoid and a home-plate region. Both are calculable and colored to assist in finding their parity vectors to aid in analysis.

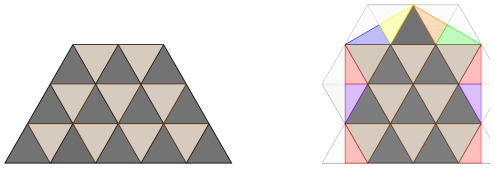

Figure 32: Two regions prepared for measurement

IV.2 A Tri-Coloring Analysis of the Tridrafters

A second method, new in design, is the *tri-coloring* method. As the name may suggest, we use three colors to give values to our tridrafters based upon these three colors. This gives us three values similar to the three variant parity method but at the same time; one for each color. We take the equilateral triangles and each of them have all three altitudes placed creating six congruent 30°-60°-90° triangles or *mini-drafters*. We then take the six triangles and color them in pairs such that the triangles with their 30° angles in the same corner are colored the same as shown in Figure 33. When the equilateral triangle is pointed upwards: the two in the upper corner are colored red, the two in the left corner are colored blue, and the two in the right corner are colored green. The downward cells are 180° rotations of the upward cells. Looking back at the cells, we see we have three kites within each cell made up of two right triangles which are given a value of 1, giving the entire kite a value of 2. We also represent these in a vector form with three components.

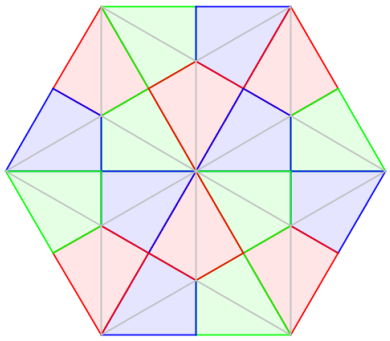

Figure 33: Tri-coloring grid

Following the same process to determine values with respect to parity, we can do the same for tri-coloring. Here, x will represent the number of red mini-drafters covered by the drafter, y for the blue, and z for the green.

Definition 13. Let R be a figure (polydrafter, region, etc.). We define t as the function that takes R and maps it to the 3-dimensional vector $\langle x, y, z \rangle$ where x, y, and z are the tri-coloring values as defined in the measuring process. We call $\langle x, y, z \rangle$ the *tri-coloring vector* of R.

T_1's tri-coloring vector $t(T_1)$, in it's shown position, would be $\langle 3, 2, 4 \rangle$. Figure 34 provides a visual.

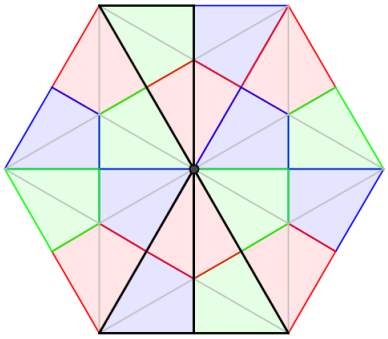

Figure 34: T_1's drafter positions on tri-coloring grid

Just as it was with our *parity* process, when performing actions σ or τ, the vector's components are altered. Unlike the parity measuring though, our numbers remain constant and shift their positions within the vector rather than being negated.

Theorem 19. *Performing action $\sigma(P)$ will alter the tri-coloring vector's measurement from $\langle x, y, z \rangle$ to $\langle z, x, y \rangle$. Given a polydrafter T with $t(T) = \langle x, y, z \rangle$, $t(\sigma(T)) = \langle y, z, x \rangle$.*

Proof. Any polydrafter may be measured through a similar process relative to Figure 34; here count the number of colored half-cells and add them to determine the appropriate colored values. If the polydrafter is rotated 60° then all drafters composing the polydrafter rotate 60°. After realigning the drafter to its new orientation; red values now rest in a green area, blue values now rest in a red area, and green values now rest in a blue area. This causes each component of the vector to shift to the left. □

Theorem 20. *Given a polydrafter T with $t(T) = \langle x, y, z \rangle$, $t(\sigma^2(T)) = \langle z, x, y \rangle$.*

Proof. Any polydrafter may be measured through a similar process given relative to Figure 34; here count the number of colored half-cells and add them to determine the appropriate colored values. If the polydrafter is rotated 120° then all drafters composing the polydrafter rotate 120°. After realigning the drafter to its new orientation; red values now rest in a blue area, blue values

now rest in a green area, and green values now rest in a red area. This causes each component of the vector to shift to the left twice. □

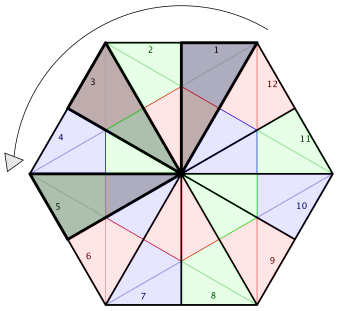

Theorem 21. *Given a polydrafter T with $t(T) = \langle x, y, z \rangle$, $t(\tau(T)) = \langle x, z, y \rangle$.*

Proof. Any polydrafter may be measured through a similar process relative to Figure 34; here count the number of colored half-cells and add them to determine the appropriate colored values. If the polydrafter is reflected vertically then all drafters composing the polydrafter are reflected as well. The red values then still rest in a red area, blue values now a green area, and green values now in a blue area. This causes the second and third components of the vector to swap locations. □

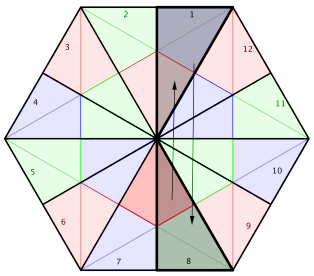

Corollary 21.1. *The tri-coloring vector of any polydrafter T can only be altered to one of six forms when performing actions σ and τ: its original $\langle x, y, z \rangle$, $\langle y, z, x \rangle$, $\langle z, x, y \rangle$, $\langle x, z, y \rangle$, $\langle y, x, z \rangle$, or $\langle z, y, x \rangle$.*

Note that a full upward and downward cell will always have 2 red mini-drafters, 2 blue mini-drafters, and 2 green mini-drafters which will always result in a tri-coloring vector of $\langle 2, 2, 2 \rangle$.

Table 2: Color values by position

Orientation	x	y	z
1	1	2	0
2	1	0	2
3	2	0	1
4	0	2	1
5	0	1	2
6	2	1	0
7	1	2	0
8	1	0	2
9	2	0	1
10	0	2	1
11	0	1	2
12	2	1	0

We can give a tri-coloring vector to any region just as we gave a parity vector before. The trapezoidal region we've worked with is composed of 21 full cells. As each cell has the tri-coloring vector of $\langle 2, 2, 2\rangle$, the region has a tri-coloring vector of $\langle 42, 42, 42\rangle$. Note that like with the parity vector, no tri-coloring vector can be given to a region such as the rhombus shown in Figure 31.

Just as we have multiple combinations to create the $\langle 6, 0, 0\rangle$ vector from our parity measurements, we have multiple combinations that create the resultant vector $\langle 42, 42, 42\rangle$. This method, on its own, also fails to prove the observed conjecture.

IV.3 Combining Measurments

Our parity vector $\langle a, b, c\rangle$ along with our tri-coloring vector $\langle x, y, z\rangle$ can be joined together to create one vector with six components, known as a *hexcomb*.

Definition 14. The *hexcomb* is the six component vector $\langle a, b, c, x, y, z \rangle$ where a, b, and c are the values from parity measuring and x, y, and z are the values from tri-color measuring.

When we perform the σ or τ action, we simply apply the individual rules for a, b, and c, and then the individual rules for x, y, and z as they have been explained previously. Table 1 shows each of the 14 tridrafters, labeled with respect to the tridrafter shapes listed in figure 13, and their measurments as its *identity* form, I.

The identity position, I, is arbitrary. One may create a table similar to Table 3 gathering the *hexcomb* values of T_1 through T_{14} with random orientations. These orientations were used such that the *hexcombs* were as similar to one another as possible. Doing so makes the observation of how the *hexcombs* change with actions a simpler task.

Table 3: I values

$I(T_n)$	a	b	c	x	y	z
T_1	1	1	-1	3	2	4
T_2	1	1	-1	3	2	4
T_3	1	3	1	5	2	2
T_4	1	1	-1	1	2	6
T_5	1	1	3	3	2	4
T_6	1	1	-1	3	2	4
T_7	1	1	-1	3	2	4
T_8	1	1	3	3	2	4
T_9	1	1	-1	3	2	4
T_{10}	1	1	-1	1	3	5
T_{11}	1	1	3	1	2	6
T_{12}	1	3	1	3	3	3
T_{13}	1	1	3	1	3	5
T_{14}	1	1	-1	3	2	4

Tables 5 through 16 located in the appendix show tables like the one above for all 12 position's values (starting with this for Table 5) for all 14 drafters.

Jost and Maor depict actions simply; through the use of a pictorial chart showing how all six portions of an equilateral triangle are formed by drawn altitudes. [6] A useful tool to this problem would be a table that shows the resultant position a shaped ends up in when we take any two actions with repetition allowed. We have a total of 12 actions that describe what position the shape is in with respect to the standard position it starts in.

1. $\sigma^m(T_n)$: The tridrafter, T_n is rotated 60° m times, $0 \geq m \geq 5$.

2. $\tau(T_n)$: The tridrafter, T_n is reflected vertically.

If we take any two random actions, repetition allowed, and perform them on any polydrafter, the polydrafter will end up in one of the twelve positions. The following table, shows every

possible pair of ordered actions and what position they result in. To find the resultant position of combining two actions, match the row to the first action performed and the column to the second action performed. The main purpose of this table is to demonstrate that any combination or actions will always result in one of the twelve originally defined positions; implying that this set of actions is closed.

For example, $\sigma^4(\tau(T_4))$ is taking T_4 in its initial position I from its position and performing a reflection followed by a total of four rotations of 60°. The resultant position can be found in the table in the seventh row and the fifth column; the result being $\sigma^2\tau$. You can also reason from this that reflecting a polydrafter followed by rotating it four times is the same as rotating the polydrafter twice and then reflecting it.

Table 4: Two actions

Action	I	σ	σ^2	σ^3	σ^4	σ^5	τ	$\sigma\tau$	$\sigma^2\tau$	$\sigma^3\tau$	$\sigma^4\tau$	$\sigma^5\tau$
I	I	σ	σ^2	σ^3	σ^4	σ^5	τ	$\sigma\tau$	$\sigma^2\tau$	$\sigma^3\tau$	$\sigma^4\tau$	$\sigma^5\tau$
σ	σ	σ^2	σ^3	σ^4	σ^5	I	$\sigma\tau$	$\sigma^2\tau$	$\sigma^3\tau$	$\sigma^4\tau$	$\sigma^5\tau$	τ
σ^2	σ^2	σ^3	σ^4	σ^5	I	σ	$\sigma^2\tau$	$\sigma^3\tau$	$\sigma^4\tau$	$\sigma^5\tau$	τ	$\sigma\tau$
σ^3	σ^3	σ^4	σ^5	I	σ	σ^2	$\sigma^3\tau$	$\sigma^4\tau$	$\sigma^5\tau$	τ	$\sigma\tau$	$\sigma^2\tau$
σ^4	σ^4	σ^5	I	σ	σ^2	σ^3	$\sigma^4\tau$	$\sigma^5\tau$	τ	$\sigma\tau$	$\sigma^2\tau$	$\sigma^3\tau$
σ^5	σ^5	I	σ	σ^2	σ^3	σ^4	$\sigma^5\tau$	τ	$\sigma\tau$	$\sigma^2\tau$	$\sigma^3\tau$	$\sigma^4\tau$
τ	τ	$\sigma^5\tau$	$\sigma^4\tau$	$\sigma^3\tau$	$\sigma^2\tau$	$\sigma\tau$	I	σ^5	σ^4	σ^3	σ^2	σ
$\sigma\tau$	$\sigma\tau$	τ	$\sigma^5\tau$	$\sigma^4\tau$	$\sigma^3\tau$	$\sigma^2\tau$	σ	I	σ^5	σ^4	σ^3	σ^2
$\sigma^2\tau$	$\sigma^2\tau$	$\sigma\tau$	τ	$\sigma^5\tau$	$\sigma^4\tau$	$\sigma^3\tau$	σ^2	σ	I	σ^5	σ^4	σ^3
$\sigma^3\tau$	$\sigma^3\tau$	$\sigma^2\tau$	$\sigma\tau$	τ	$\sigma^5\tau$	$\sigma^4\tau$	σ^3	σ^2	σ	I	σ^5	σ^4
$\sigma^4\tau$	$\sigma^4\tau$	$\sigma^3\tau$	$\sigma^2\tau$	$\sigma\tau$	τ	$\sigma^5\tau$	σ^4	σ^3	σ^2	σ	I	σ^5
$\sigma^5\tau$	$\sigma^5\tau$	$\sigma^4\tau$	$\sigma^3\tau$	$\sigma^2\tau$	$\sigma\tau$	τ	σ^5	σ^4	σ^3	σ^2	σ	I

Looking closely, we see that this is the dihedral group with 12 elements, D_6. We will take it and make two more. These will be copies of Table 4 with all actions that cause the same resultant vector form written in the same color. Table 5 is colored for the parity vectors and table 6 is colored

for the tri-coloring vectors.

Table 5: Two action parity

Action	I	σ	σ^2	σ^3	σ^4	σ^5	τ	$\sigma\tau$	$\sigma^2\tau$	$\sigma^3\tau$	$\sigma^4\tau$	$\sigma^5\tau$
I	I	σ	σ^2	σ^3	σ^4	σ^5	τ	$\sigma\tau$	$\sigma^2\tau$	$\sigma^3\tau$	$\sigma^4\tau$	$\sigma^5\tau$
σ	σ	σ^2	σ^3	σ^4	σ^5	I	$\sigma\tau$	$\sigma^2\tau$	$\sigma^3\tau$	$\sigma^4\tau$	$\sigma^5\tau$	τ
σ^2	σ^2	σ^3	σ^4	σ^5	I	σ	$\sigma^2\tau$	$\sigma^3\tau$	$\sigma^4\tau$	$\sigma^5\tau$	τ	$\sigma\tau$
σ^3	σ^3	σ^4	σ^5	I	σ	σ^2	$\sigma^3\tau$	$\sigma^4\tau$	$\sigma^5\tau$	τ	$\sigma\tau$	$\sigma^2\tau$
σ^4	σ^4	σ^5	I	σ	σ^2	σ^3	$\sigma^4\tau$	$\sigma^5\tau$	τ	$\sigma\tau$	$\sigma^2\tau$	$\sigma^3\tau$
σ^5	σ^5	I	σ	σ^2	σ^3	σ^4	$\sigma^5\tau$	τ	$\sigma\tau$	$\sigma^2\tau$	$\sigma^3\tau$	$\sigma^4\tau$
τ	τ	$\sigma^5\tau$	$\sigma^4\tau$	$\sigma^3\tau$	$\sigma^2\tau$	$\sigma\tau$	I	σ^5	σ^4	σ^3	σ^2	σ
$\sigma\tau$	$\sigma\tau$	τ	$\sigma^5\tau$	$\sigma^4\tau$	$\sigma^3\tau$	$\sigma^2\tau$	σ	I	σ^5	σ^4	σ^3	σ^2
$\sigma^2\tau$	$\sigma^2\tau$	$\sigma\tau$	τ	$\sigma^5\tau$	$\sigma^4\tau$	$\sigma^3\tau$	σ^2	σ	I	σ^5	σ^4	σ^3
$\sigma^3\tau$	$\sigma^3\tau$	$\sigma^2\tau$	$\sigma\tau$	τ	$\sigma^5\tau$	$\sigma^4\tau$	σ^3	σ^2	σ	I	σ^5	σ^4
$\sigma^4\tau$	$\sigma^4\tau$	$\sigma^3\tau$	$\sigma^2\tau$	$\sigma\tau$	τ	$\sigma^5\tau$	σ^4	σ^3	σ^2	σ	I	σ^5
$\sigma^5\tau$	$\sigma^5\tau$	$\sigma^4\tau$	$\sigma^3\tau$	$\sigma^2\tau$	$\sigma\tau$	τ	σ^5	$I\sigma^4$	σ^3	σ^2	σ	I

Table 6: Two actions tri-coloring

Action	I	σ	σ^2	σ^3	σ^4	σ^5	τ	$\sigma\tau$	$\sigma^2\tau$	$\sigma^3\tau$	$\sigma^4\tau$	$\sigma^5\tau$
I	I	σ	σ^2	σ^3	σ^4	σ^5	τ	$\sigma\tau$	$\sigma^2\tau$	$\sigma^3\tau$	$\sigma^4\tau$	$\sigma^5\tau$
σ	σ	σ^2	σ^3	σ^4	σ^5	I	$\sigma\tau$	$\sigma^2\tau$	$\sigma^3\tau$	$\sigma^4\tau$	$\sigma^5\tau$	τ
σ^2	σ^2	σ^3	σ^4	σ^5	I	σ	$\sigma^2\tau$	$\sigma^3\tau$	$\sigma^4\tau$	$\sigma^5\tau$	τ	$\sigma\tau$
σ^3	σ^3	σ^4	σ^5	I	σ	σ^2	$\sigma^3\tau$	$\sigma^4\tau$	$\sigma^5\tau$	τ	$\sigma\tau$	$\sigma^2\tau$
σ^4	σ^4	σ^5	I	σ	σ^2	σ^3	$\sigma^4\tau$	$\sigma^5\tau$	τ	$\sigma\tau$	$\sigma^2\tau$	$\sigma^3\tau$
σ^5	σ^5	I	σ	σ^2	σ^3	σ^4	$\sigma^5\tau$	τ	$\sigma\tau$	$\sigma^2\tau$	$\sigma^3\tau$	$\sigma^4\tau$
τ	τ	$\sigma^5\tau$	$\sigma^4\tau$	$\sigma^3\tau$	$\sigma^2\tau$	$\sigma\tau$	I	σ^5	σ^4	σ^3	σ^2	σ
$\sigma\tau$	$\sigma\tau$	τ	$\sigma^5\tau$	$\sigma^4\tau$	$\sigma^3\tau$	$\sigma^2\tau$	σ	I	σ^5	σ^4	σ^3	σ^2
$\sigma^2\tau$	$\sigma^2\tau$	$\sigma\tau$	τ	$\sigma^5\tau$	$\sigma^4\tau$	$\sigma^3\tau$	σ^2	σ	I	σ^5	σ^4	σ^3
$\sigma^3\tau$	$\sigma^3\tau$	$\sigma^2\tau$	$\sigma\tau$	τ	$\sigma^5\tau$	$\sigma^4\tau$	σ^3	σ^2	σ	I	σ^5	σ^4
$\sigma^4\tau$	$\sigma^4\tau$	$\sigma^3\tau$	$\sigma^2\tau$	$\sigma\tau$	τ	$\sigma^5\tau$	σ^4	σ^3	σ^2	σ	I	σ^5
$\sigma^5\tau$	$\sigma^5\tau$	$\sigma^4\tau$	$\sigma^3\tau$	$\sigma^2\tau$	$\sigma\tau$	τ	σ^5	σ^4	σ^3	σ^2	σ	I

Again, table 4 has the same symmetry as the dihedral group D_6. What this tells us is that no matter which of our original 12 actions we take and combine with any other action, we never end up with a result that couldn't be made with a single one of those original actions in the first place. Applying each action once to each drafter and measuring its hexcomb yields all possible forms the polydrafter may be expressed in.
Finding the hexcomb of a specific region is simply combining the parity and tri-coloring vectors for said region together.

With the knowledge of our 12 possible single actions already relaying the results of any combination of actions, one is able to come to the question "What are all possible results $\langle a, b, c, x, y, z\rangle$ with all 14 pieces being measured in every possible position?". As there are 14 pieces with 12 possible positions there are 12^{14} or 56, 693, 912, 375, 296 potential unique hexcombs.

Using Mathlab and the RIT Cluster Network, all possible results were calculated. The coding is provided for the reader in the appendix, 8.3, as well as a list of all the unique solutions

amounting to 2,425,846.

V. Measuring Solutions

V.1 Hexcombs of Solutions

Each of the 75 convex shapes that can be created using the 14 tridrafters potentially have a hexcomb to describe it. The following procedure explains how the potential hexcombs were found.

1. Take the outline of the region and place it so at least one side conforms to the triangular grid.
2. Move the outline around such that as many sides as possible conform to the triangular grid or the altitudes of the triangles that make up the grid simultaneously.
3. If it is possible to have all sides conform simultaneously, find the hexcomb that defines the shape.
4. If it is not possible to have all sides conform simultaneously, the shape has no parity or tri-coloring vector, and thus cannot be given a hexcomb.

Like the rhombus from Figure 31, if the entirety of the region can't conform to cell borders, the region can not be assigned a hexcomb value as it has no parity vector or tri-coloring vector to describe it.

For those regions that can be placed upon the grid such that a hexcomb can be measured, we find it. We find the hexcomb with the following procedure.

1. Place the region upon the grid such that all sides of the shape are bound by the triangular grid or the trangle's altitudes.
2. Color all equilateral triangles that point upwards black.
   (a) Each black cell has a value of $\langle 2, 0, 0, 2, 2, 2 \rangle$
3. Color all equilateral triangles that point downwards grey.
   (a) Each grey cell has a value of $\langle -2, 0, 0, 2, 2, 2 \rangle$

4. Color all right triangles created from an altitude drawn from the top of equilateral tringles that points upwards red; there are two potential positions: 7 and 8.
   (a) Position 7 has a value of $\langle 1, 1, 1, 1, 2, 0 \rangle$
   (b) Position 8 has a value of $\langle 1, -1, -1, 1, 0, 2 \rangle$
5. Color all right triangles created from an altitude drawn from the bottom of equilateral tringles that points downwards purple; there are two potential positions: 2 and 1.
   (a) Position 2 has a value of $\langle -1, -1, 1, 1, 0, 2 \rangle$
   (b) Position 1 has a value of $\langle -1, 1, -1, 1, 2, 0 \rangle$
6. Color all right triangles created from an altitude drawn from the left of equilateral tringles that points upwards blue; there are two potential positions: 12 and 11.
   (a) Position 12 has a value of $\langle 1, -1, -1, 2, 1, 0 \rangle$
   (b) Position 11 has a value of $\langle 1, 1, 1, 0, 1, 2 \rangle$
7. Color all right triangles created from an altitude drawn from the right of equilateral tringles that points downwards yellow; there are two potential positions: 5 and 6.
   (a) Position 5 has a value of $\langle -1, 1, -1, 0, 1, 2 \rangle$
   (b) Position 6 has a value of $\langle -1, -1, 1, 2, 1, 0 \rangle$
8. Color all right triangles created from an altitude drawn from the right of equilateral tringles that points upwards green; there are two potential positions: 4 and 3.
   (a) Position 4 has a value of $\langle 1, -1, -1, 0, 2, 1 \rangle$
   (b) Position 3 has a value of $\langle 1, 1, 1, 2, 0, 1 \rangle$
9. Color all right triangles created from an altitude drawn from the left of equilateral tringles that points downwards orange; there are two potential positions: 9 and 10.
   (a) Position 9 has a value of $\langle -1, 1, -1, 2, 0, 1 \rangle$
   (b) Position 10 has a value of $\langle -1, -1, 1, 0, 2, 1 \rangle$

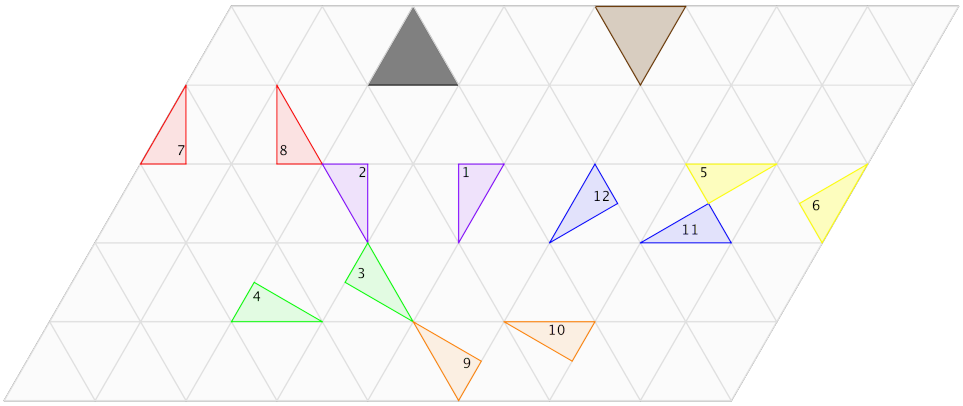

Figure 35: Hexcomb measuring table

10. Add each value of each existing region to obtain the value of the region's hexcomb.

The hexcombs for each of these positions can be verified by the reader. Figure 35 helps to show the coloring of each position to aid in this.

Two examples of calculating hexcombs with the aforementioned process are applied to the regions shown in Figure 36; the trapezoid and "home-plate" shaped region.

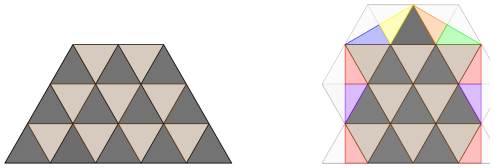

Figure 36: Coloring for hexcomb values

The trapezoid has a total of eight black regions and nine grey regions. $12 * \langle 2,0,0,2,2,2\rangle + 9 * \langle -2,0,0,2,2,2\rangle = \langle 6,0,0,42,42,42\rangle$

The "home-plate" region has a total of eight black cells, eight grey cells, two position 7 right triangles, two position 8 right triangles, one position 2 right triangle, one position 1 right triangle, one position 11 right triangle, one position 6 right triangle, one position 4 right triangle, and one position 9 right triangle. $8 * \langle 2,0,0,2,2,2\rangle + 8 * \langle -2,0,0,2,2,2\rangle + 2 * \langle 1,1,1,1,2,0\rangle + 2 * \langle 1,-1,-1,1,0,2\rangle + \langle -1,-1,1,1,0,2\rangle + \langle -1,1,-1,1,2,0\rangle + \langle 1,1,1,0,1,2\rangle + \langle -1,-1,1,2,1,0\rangle + \langle 1,-1,-1,0,2,1\rangle + \langle -1,1,-1,2,0,1\rangle = \langle 2,0,0,42,42,42\rangle$

These two resultant hexcombs describe region 73 and region 45 respectively.

Every Region that could be measured was and the following list of hexcombs were found. VIII.4 in the appendix gives the regions colored in the aforementioned process to determine these.

1. Region 1 $\langle 2, 0, 0, 41, 44, 41 \rangle$
2. Region 4 $\langle 2, 0, 0, 42, 42, 42 \rangle$
3. Region 6 $\langle 2, 0, -4, 42, 42, 42 \rangle$
4. Region 7 $\langle 2, 0, 8, 42, 42, 42 \rangle$
5. Region 8 $\langle 0, 0, 2, 42, 42, 42 \rangle$
6. Region 10 $\langle 2, 0, 0, 42, 42, 42 \rangle$
7. Region 16 $\langle -2, 0, 0, 44, 41, 41 \rangle$
8. Region 19 $\langle 2, 0, 8, 42, 42, 42 \rangle$
9. Region 33 $\langle 0, 0, -2, 42, 42, 42 \rangle$
10. Region 35 $\langle 0, 0, 2, 42, 42, 42 \rangle$
11. Region 36 $\langle 0, 0, -2, 42, 42, 42 \rangle$
12. Region 37 $\langle 2, 0, 4, 42, 42, 42 \rangle$
13. Region 38 $\langle 2, 0, 4, 42, 42, 42 \rangle$
14. Region 40 $\langle 6, 0, 0, 42, 42, 42 \rangle$
15. Region 45 $\langle 2, 0, 0, 42, 42, 42 \rangle$
16. Region 47 $\langle 2, 0, 4, 42, 42, 42 \rangle$
17. Region 48 $\langle 2, 0, 0, 42, 42, 42 \rangle$
18. Region 54 $\langle 0, 0, -6, 43, 40, 43 \rangle$
19. Region 57 $\langle 2, 0, -4, 42, 42, 42 \rangle$

20. Region 58 $\langle 4, 0, -6, 42, 42, 42 \rangle$
21. Region 59 $\langle 2, 0, 4, 42, 42, 42 \rangle$
22. Region 60 $\langle 2, 0, -4, 42, 42, 42 \rangle$
23. Region 61 $\langle 2, 0, 0, 42, 42, 42 \rangle$
24. Region 62 $\langle 6, 0, 4, 42, 42, 42 \rangle$
25. Region 63 $\langle 2, 0, 0, 42, 42, 42 \rangle$
26. Region 65 $\langle 4, 2, 4, 43, 42, 41 \rangle$
27. Region 70 $\langle 4, 0, -2, 42, 42, 42 \rangle$
28. Region 71 $\langle 4, 0, 6, 42, 42, 42 \rangle$
29. Region 73 $\langle 6, 0, 0, 42, 42, 42 \rangle$
30. Region 74 $\langle 4, 0, -2, 42, 42, 42 \rangle$

Every region, for which a hexcomb can be found, is shown colored in Appendix 8.4.

VI. Conclusion

Although the methods outlined in this paper do not prove the conjecture, they may be expanded upon and be helpful with other tiling problems; offering a different method analysis. With respect to this paper's conjecture, these methods give strong evidence as it gives proof to why particular regions, those not shown VIII.4, must exhibit this property due to the nature of their border's positioning. Additionally, there are theorems and arguments that give more credence to the conjecture which were independently made without the influence of knowing of the solutions to all convex regions in advance.

Parity is a tool that is already fairly simple to utilize with the value of two or halves. The method of "Tri-coloring" introduced in this paper is a technique that may yet be applied to other puzzles that are more hexagonal in nature or have the property of being divided into thirds relatively simply. Puzzles and problems that utilize a set of polygons with a base closely related to triangles such as drafters and polyiamonds discussed and shown in this paper; rhombuses or trapezoids which are closely related to hexagons; etc.

Overall, with two failures of proof, it seems that proving the necessity of the against-the-grain property using combinatorics through the means of values provided through or similar to parity is ineffective. Additional values may be utilized, but if intended to be used in union with parity and tri-coloring will cause greater complexity as the calculation of new vectors will grow in complexity.

VII. ACKNOWLEDGEMENTS

Firstly, I would like to thank my thesis advisor Dr. Matthew Coppenbarger of the Math Department at the Rochester Institute of Technology. Open office and holiday hours of time were given to me a multitude of times to assist me in ensuring not only this paper's content, but its clarity.

I would also like to thank Ross Delinger and Josh McSavaney who assisted in the running of my programs utilizing R.I.T.'s cluster network to provide me with the results of my programming.

I would also like to acknowledge Dr. Hossein Shahmohamad, Dr. Darren Narayan, and Dr. David Ross as second readers of this thesis; I am gratefully indebted to their astute comments upon this thesis.

Finally, I must offer my finest gratitude to my parents, Dr. Eileen Watson and Mr. Greg Garten, for their perpetual support and encouragement through the entirety of my academic career. Also my close friends Mr. Jonathan Casillas, Mr. Sean Fitzgerald, and Ms. Courtney Fitzgerald for their assistance regarding programming languages and the establishment of logical arguments. This accomplishment would not have been possible without them. Thank you.

Trevor Nelson

VIII. Appendix

VIII.1 Closing Graphs

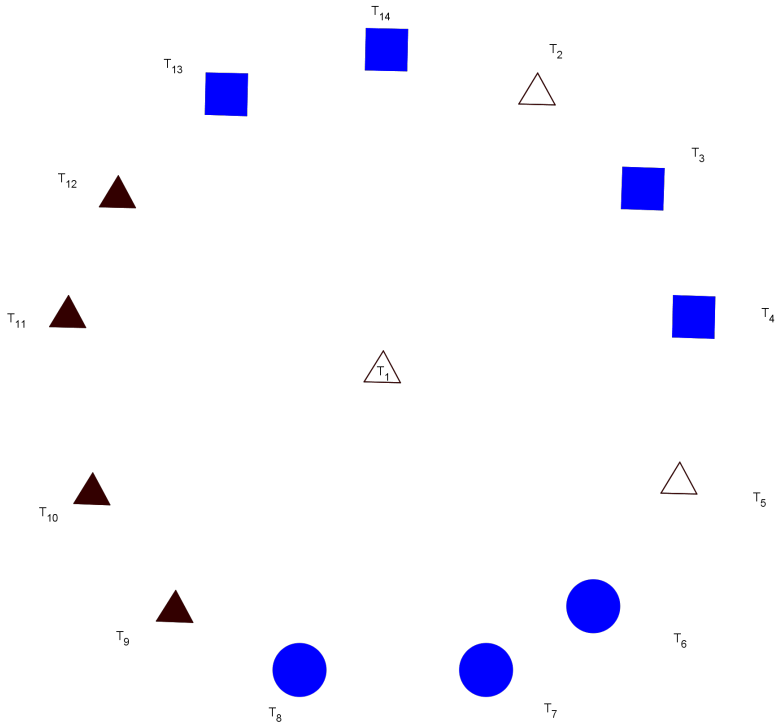

Figure 37: Closing T_1

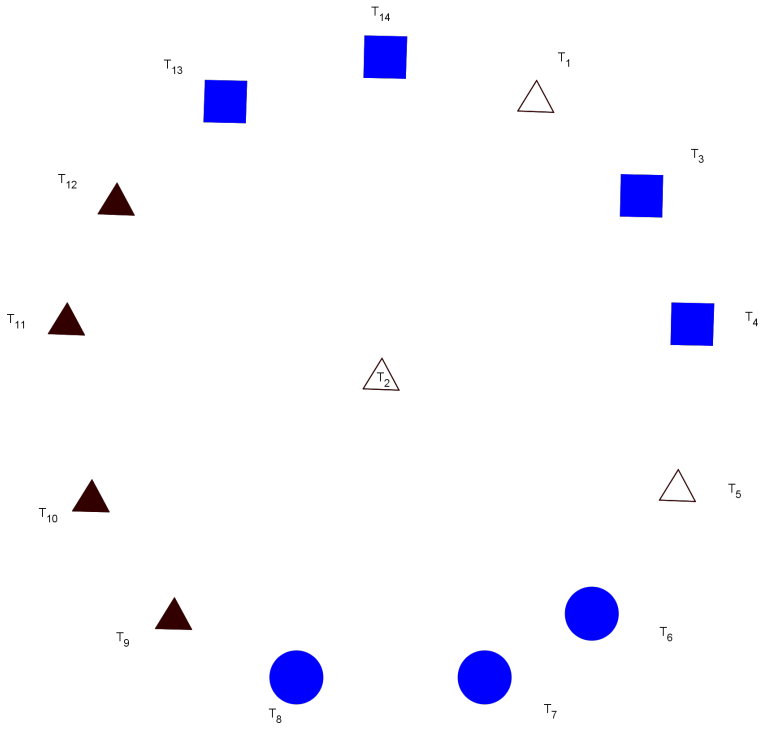

Figure 38: T_2

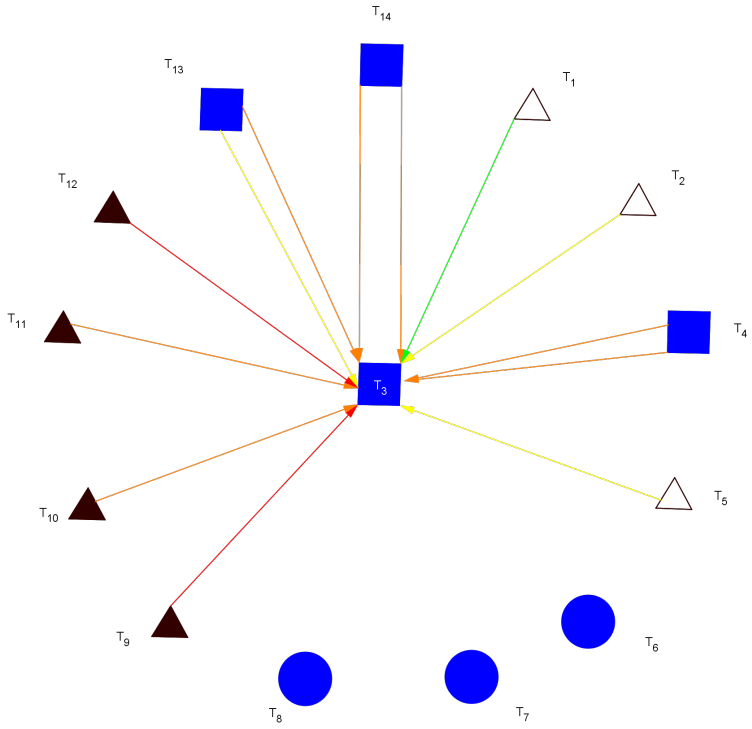

Figure 39: Closing T_3

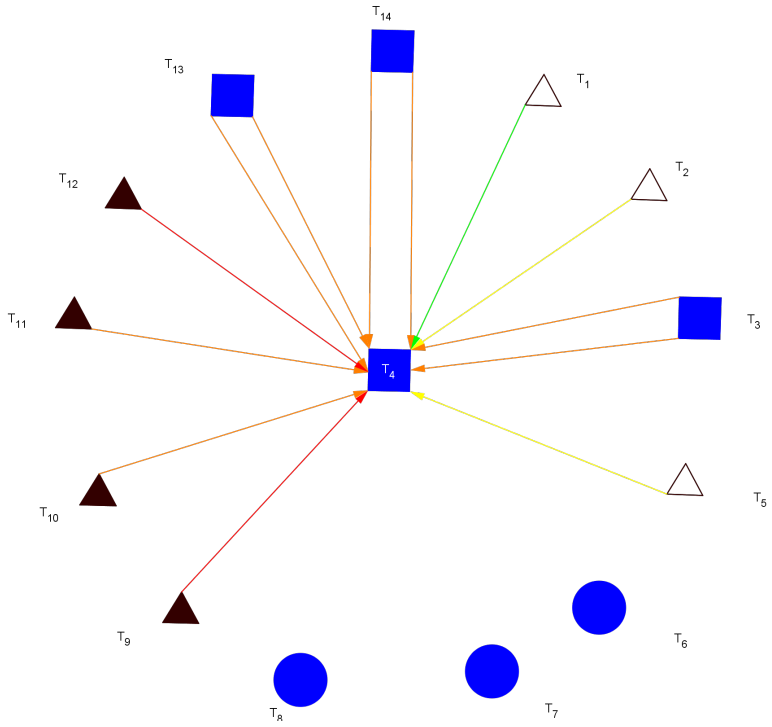

Figure 40: Closing T_4

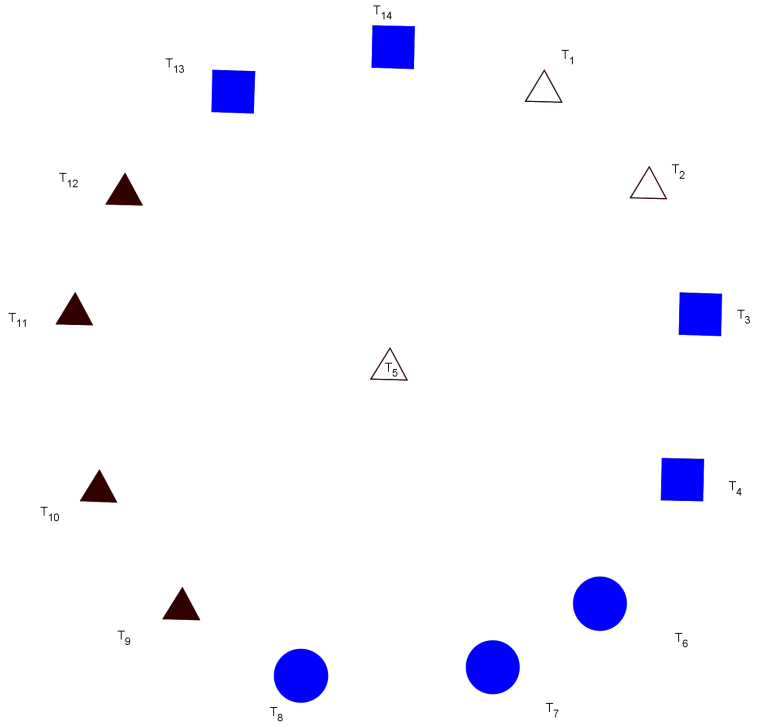

Figure 41: Closing T_5

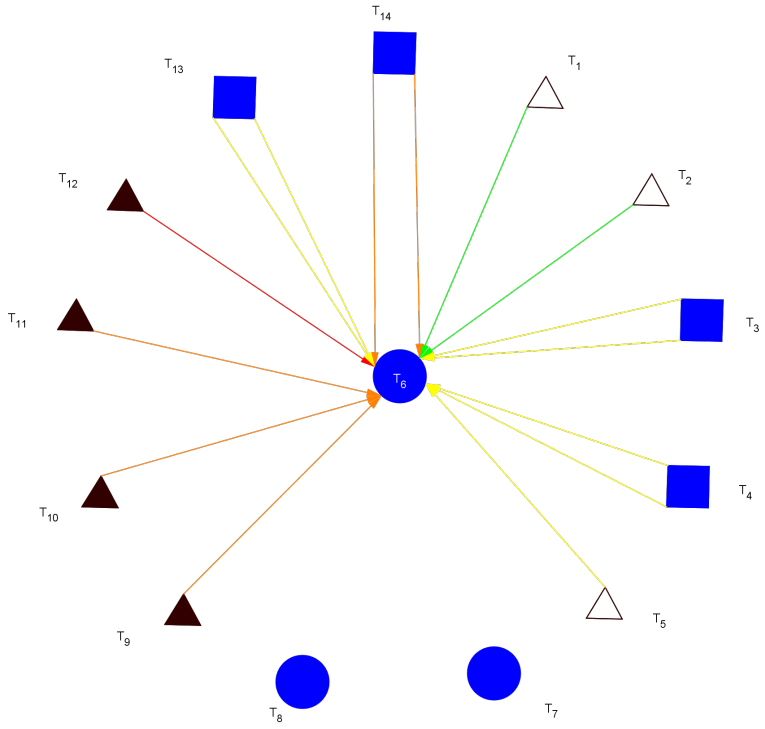

Figure 42: Closing T_6

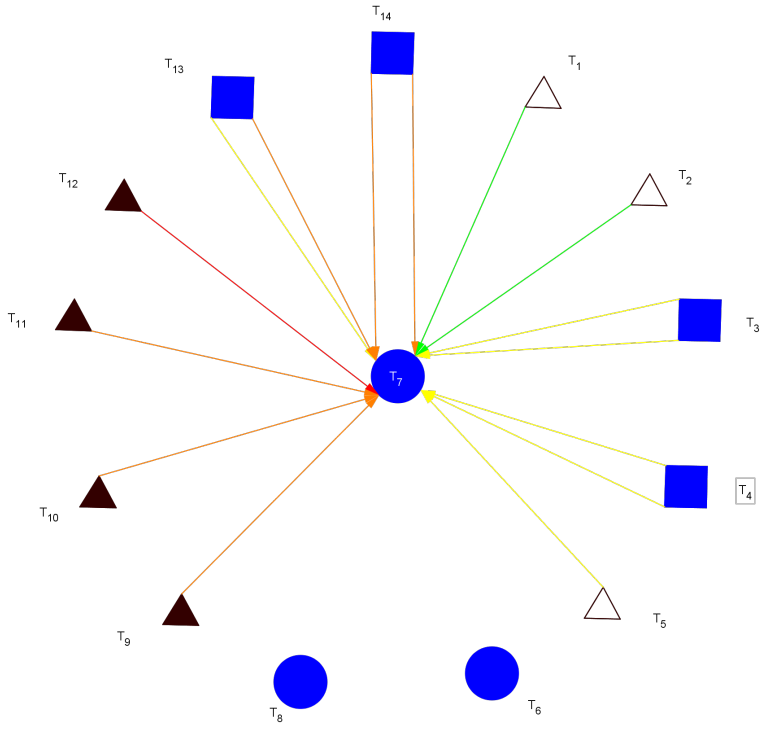

Figure 43: Closing T_7

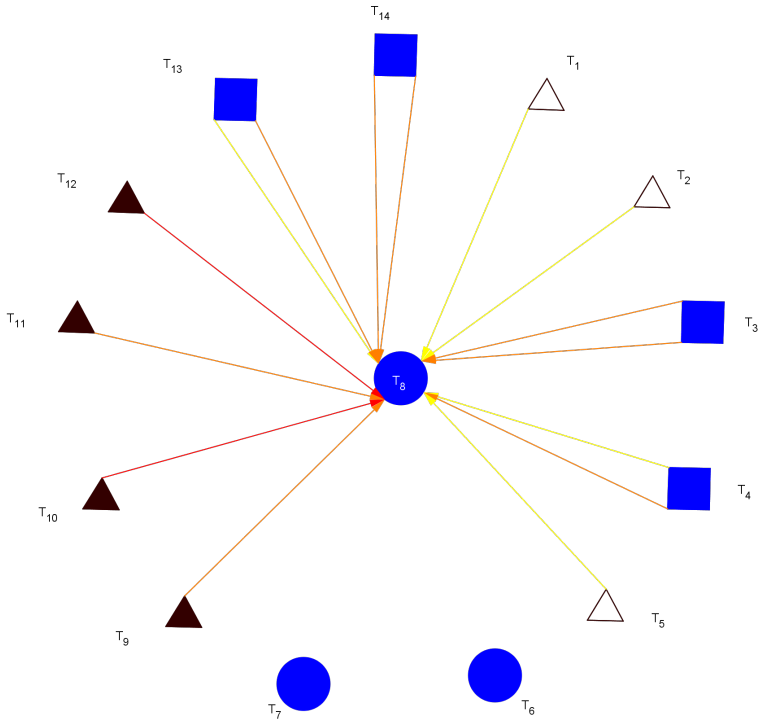

Figure 44: Closing T_8

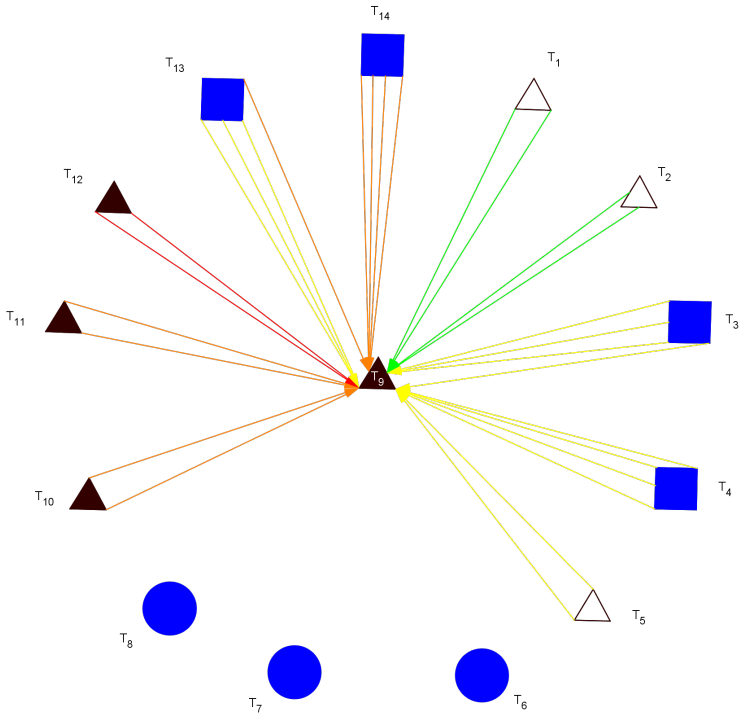

Figure 45: Closing T_9

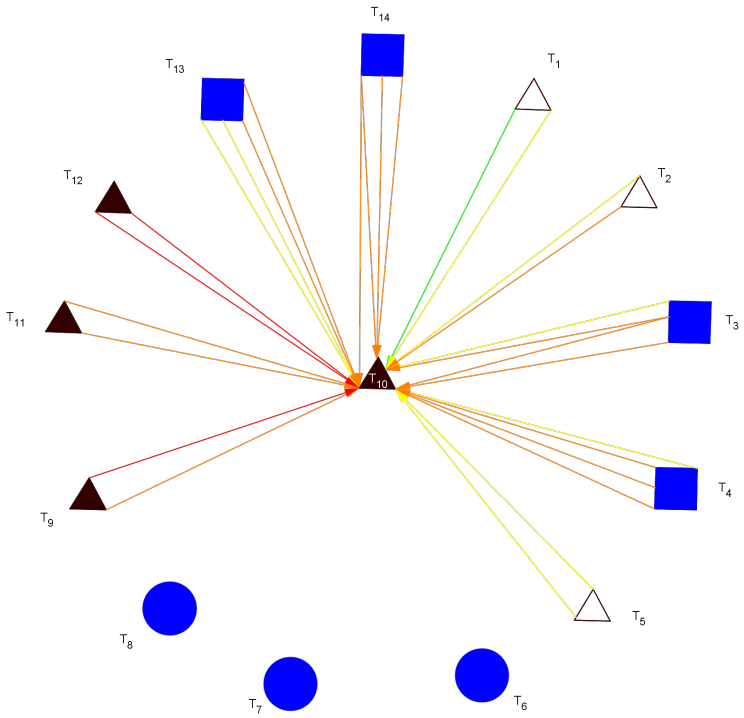

Figure 46: Closing T_{10}

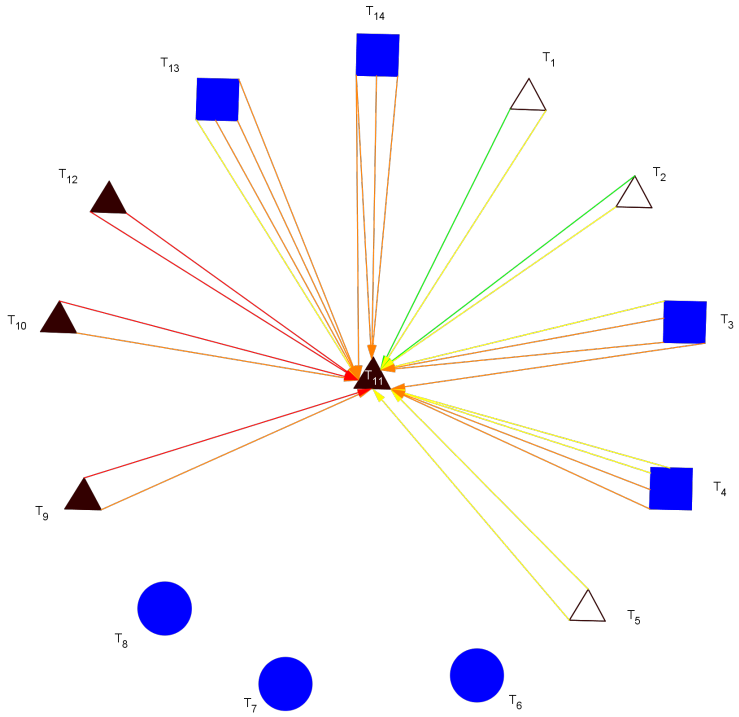

Figure 47: Closing T_{11}

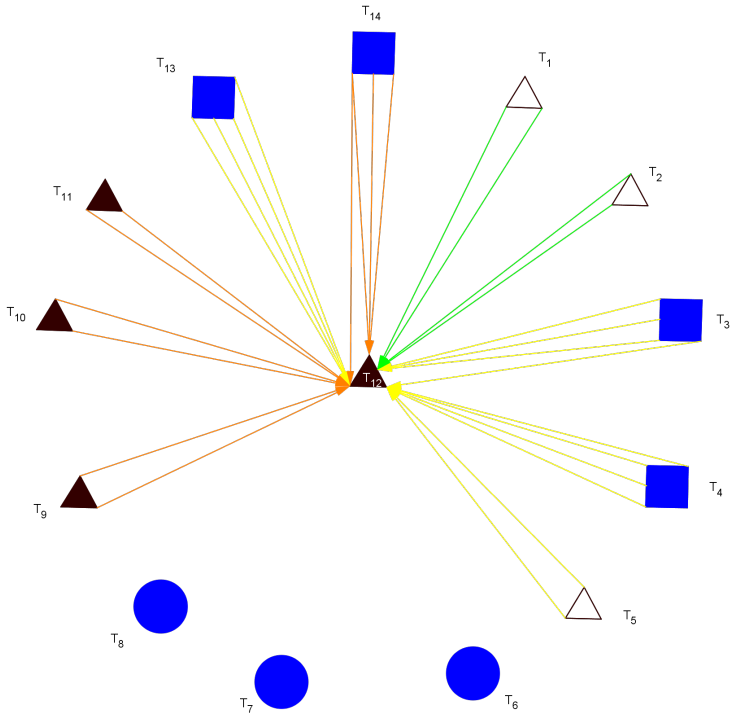

Figure 48: Closing T_{12}

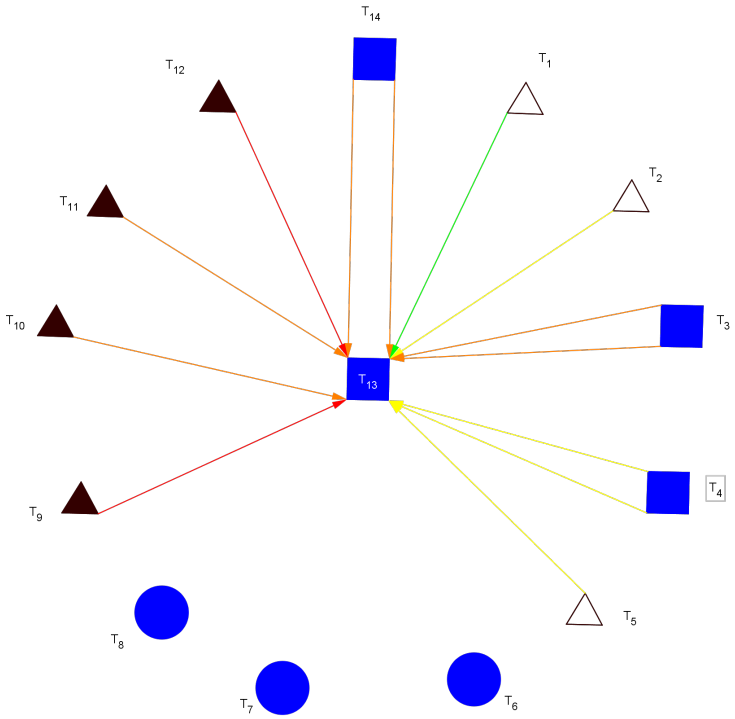

Figure 49: Closing T_{13}

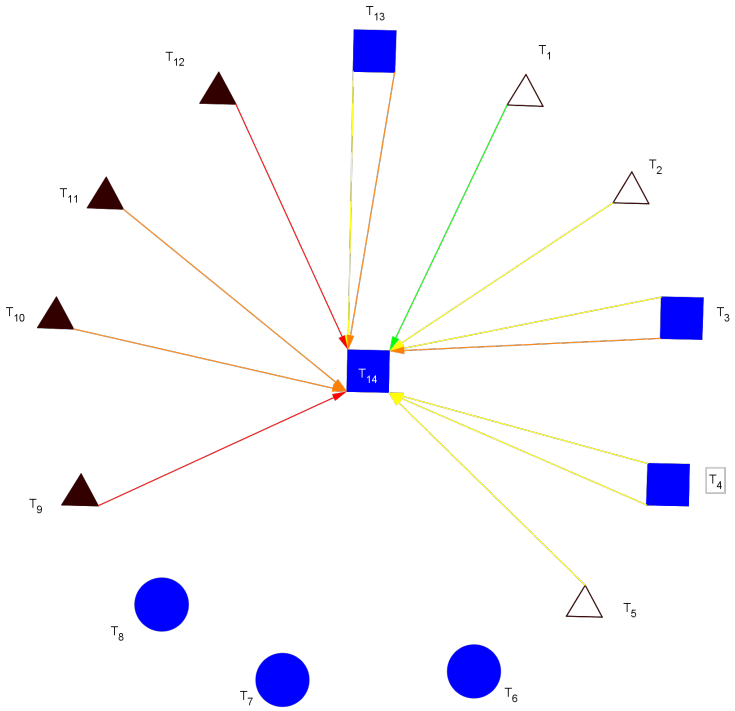

Figure 50: Closing T_{14}

VIII.2 Tridrafter Vectors In All Positions

Table 7: Identity hexcombs

$I(T_n)$	a	b	c	x	y	z
T_1	1	1	-1	3	2	4
T_2	1	1	-1	3	2	4
T_3	1	3	1	5	2	2
T_4	1	1	-1	1	2	6
T_5	1	1	3	3	2	4
T_6	1	1	-1	3	2	4
T_7	1	1	-1	3	2	4
T_8	1	1	3	3	2	4
T_9	1	1	-1	3	2	4
T_{10}	1	1	-1	1	3	5
T_{11}	1	1	3	1	2	6
T_{12}	1	3	1	3	3	3
T_{13}	1	1	3	1	3	5
T_{14}	1	1	-1	3	2	4

Table 8: σ hexcombs

$\sigma(T_n)$	a	b	c	x	y	z
T_1	-1	1	1	2	4	3
T_2	-1	1	1	2	4	3
T_3	-1	3	-1	2	2	5
T_4	-1	1	1	2	6	1
T_5	-1	1	-3	2	4	3
T_6	-1	1	1	2	4	3
T_7	-1	1	1	2	4	3
T_8	-1	1	-3	2	4	3
T_9	-1	1	1	2	4	3
T_{10}	-1	1	1	3	5	1
T_{11}	-1	1	-3	2	6	1
T_{12}	-1	3	-1	3	3	3
T_{13}	-1	1	-3	3	5	1
T_{14}	-1	1	1	2	4	3

Table 9: σ^2 hexcombs

$\sigma^2(T_n)$	a	b	c	x	y	z
T_1	1	1	-1	4	3	2
T_2	1	1	-1	4	3	2
T_3	1	3	1	2	5	2
T_4	1	1	-1	6	1	2
T_5	1	1	3	4	3	2
T_6	1	1	-1	4	3	2
T_7	1	1	-1	4	3	2
T_8	1	1	3	4	3	2
T_9	1	1	-1	4	3	2
T_{10}	1	1	-1	5	1	3
T_{11}	1	1	3	6	1	2
T_{12}	1	3	1	3	3	3
T_{13}	1	1	3	5	1	3
T_{14}	1	1	-1	4	3	2

Table 10: σ^3 hexcombs

$\sigma^3(T_n)$	a	b	c	x	y	z
T_1	-1	1	1	3	2	4
T_2	-1	1	1	3	2	4
T_3	-1	3	-1	5	2	2
T_4	-1	1	1	1	2	6
T_5	-1	1	-3	3	2	4
T_6	-1	1	1	3	2	4
T_7	-1	1	1	3	2	4
T_8	-1	1	-3	3	2	4
T_9	-1	1	1	3	2	4
T_{10}	-1	1	1	1	3	5
T_{11}	-1	1	-3	1	2	6
T_{12}	-1	3	-1	3	3	3
T_{13}	-1	1	-3	1	3	5
T_{14}	-1	1	1	3	2	4

Table 11: σ^4 hexcombs

$\sigma^4(T_n)$	a	b	c	x	y	z
T_1	1	1	-1	2	4	3
T_2	1	1	-1	2	4	3
T_3	1	3	1	2	2	5
T_4	1	1	-1	2	6	1
T_5	1	1	3	2	4	3
T_6	1	1	-1	2	4	3
T_7	1	1	-1	2	4	3
T_8	1	1	3	2	4	3
T_9	1	1	-1	2	4	3
T_{10}	1	1	-1	3	5	1
T_{11}	1	1	3	2	6	1
T_{12}	1	3	1	3	3	3
T_{13}	1	1	3	3	5	1
T_{14}	1	1	-1	2	4	3

Table 12: σ^5 hexcombs

$\sigma^5(T_n)$	a	b	c	x	y	z
T_1	-1	1	1	4	3	2
T_2	-1	1	1	4	3	2
T_3	-1	3	-1	2	5	2
T_4	-1	1	1	6	1	2
T_5	-1	1	-3	4	3	2
T_6	-1	1	1	4	3	2
T_7	-1	1	1	4	3	2
T_8	-1	1	-3	4	3	2
T_9	-1	1	1	4	3	2
T_{10}	-1	1	1	5	1	3
T_{11}	-1	1	-3	6	1	2
T_{12}	-1	3	-1	3	3	3
T_{13}	-1	1	-3	5	1	3
T_{14}	-1	1	1	4	3	2

Table 13: τ hexcombs

$\tau(T_n)$	a	b	c	x	y	z
T_1	-1	-1	-1	3	4	2
T_2	-1	-1	-1	3	4	2
T_3	-1	-3	1	5	2	2
T_4	-1	-1	-1	1	6	2
T_5	-1	-1	3	3	4	2
T_6	-1	-1	-1	3	4	2
T_7	-1	-1	-1	3	4	2
T_8	-1	-1	3	3	4	2
T_9	-1	-1	-1	3	4	2
T_{10}	-1	-1	-1	1	5	3
T_{11}	-1	-1	3	1	6	2
T_{12}	-1	-3	1	3	3	3
T_{13}	-1	-1	3	1	5	3
T_{14}	-1	-1	-1	3	4	2

Table 14: $\sigma\tau$ hexcombs

$\sigma(\tau(T_n))$	a	b	c	x	y	z
T_1	1	-1	1	2	3	4
T_2	1	-1	1	2	3	4
T_3	1	-3	-1	2	5	2
T_4	1	-1	1	2	1	6
T_5	1	-1	-3	2	3	4
T_6	1	-1	1	2	3	4
T_7	1	-1	1	2	3	4
T_8	1	-1	-3	2	3	4
T_9	1	-1	1	2	3	4
T_{10}	1	-1	1	3	1	5
T_{11}	1	-1	-3	2	1	6
T_{12}	1	-3	-1	3	3	3
T_{13}	1	-1	-3	3	1	5
T_{14}	1	-1	1	2	3	4

Table 15: $\sigma^2\tau$ hexcombs

$\sigma^2(\tau(T_n))$	a	b	c	x	y	z
T_1	-1	-1	-1	4	2	3
T_2	-1	-1	-1	4	2	3
T_3	-1	-3	1	2	2	5
T_4	-1	-1	-1	6	2	1
T_5	-1	-1	3	4	2	3
T_6	-1	-1	-1	4	2	3
T_7	-1	-1	-1	4	2	3
T_8	-1	-1	3	4	2	3
T_9	-1	-1	-1	4	2	3
T_{10}	-1	-1	-1	5	3	1
T_{11}	-1	-1	3	6	2	1
T_{12}	-1	-3	1	3	3	3
T_{13}	-1	-1	3	5	3	1
T_{14}	-1	-1	-1	4	2	3

Table 16: $\sigma^3\tau$ hexcombs

$\sigma^3(\tau(T_n))$	a	b	c	x	y	z
T_1	1	-1	1	3	4	2
T_2	1	-1	1	3	4	2
T_3	1	-3	-1	5	2	2
T_4	1	-1	1	1	6	2
T_5	1	-1	-3	3	4	2
T_6	1	-1	1	3	4	2
T_7	1	-1	1	3	4	2
T_8	1	-1	-3	3	4	2
T_9	1	-1	1	3	4	2
T_{10}	1	-1	1	1	5	3
T_{11}	1	-1	-3	1	6	2
T_{12}	1	-3	-1	3	3	3
T_{13}	1	-1	-3	1	5	3
T_{14}	1	-1	1	3	4	2

Table 17: $\sigma^4\tau$ hexcombs

$\sigma^4(\tau(T_n))$	a	b	c	x	y	z
T_1	-1	-1	-1	2	3	4
T_2	-1	-1	-1	2	3	4
T_3	-1	-3	1	2	5	2
T_4	-1	-1	-1	2	1	6
T_5	-1	-1	3	2	3	4
T_6	-1	-1	-1	2	3	4
T_7	-1	-1	-1	2	3	4
T_8	-1	-1	3	2	3	4
T_9	-1	-1	-1	2	3	4
T_{10}	-1	-1	-1	3	1	5
T_{11}	-1	-1	3	2	1	6
T_{12}	-1	-3	1	3	3	3
T_{13}	-1	-1	3	3	1	5
T_{14}	-1	-1	-1	2	3	4

Table 18: $\sigma^5\tau$ hexcombs

$\sigma^5(\tau(T_n))$	a	b	c	x	y	z
T_1	1	-1	1	4	2	3
T_2	1	-1	1	4	2	3
T_3	1	-3	-1	2	2	5
T_4	1	-1	1	6	2	1
T_5	1	-1	-3	4	2	3
T_6	1	-1	1	4	2	3
T_7	1	-1	1	4	2	3
T_8	1	-1	-3	4	2	3
T_9	1	-1	1	4	2	3
T_{10}	1	-1	1	5	3	1
T_{11}	1	-1	-3	6	2	1
T_{12}	1	-3	-1	3	3	3
T_{13}	1	-1	-3	5	3	1
T_{14}	1	-1	1	4	2	3

VIII.3 List of unique hexcombs

A list of all generated hexcombs are available at request; contact the author if desired.

VIII.4 Program Usage

Two different softwares were utilized to obtain the list of unique hexcombs. Mathematica and the R.I.T. Cluster Network using slurm. The codes used for each individual softwares are shown in the two respective subsections.

VIII.4.1 Mathematica Program

α Combinations- The alpha combination results were obtained with the following Mathematica code. There are 6 tridrafters that were identical when measured to $\{1, 1, -1, 3, 2, 4\}$ at R_0, tridrafers T_1, T_2, T_6, T_7, T_9, and T_{14}.

Step One

This code gives all possible results from picking any three random positions, with repetition, for any three of these pieces.

```
ClearAll
List1 = Import[ "//Volumes//NO NAME//Thesis Work//New Program//Test Union//Type Alpha.txt", "CSV"]; FinalList = { }

    For[a = 1, a <= Length[List1], a++,
For[b = 1, b <= Length[List1], b++,
For[c = 1, c <= Length[List1], c++,

    FinalList = Append[FinalList, ToExpression[List1[[a]]] + ToExpression[List1[[b]]] + ToExpression[List1[[c]]]]]]] FinalList = DeleteDuplicates[FinalList]

    Export["//Volumes//NO NAME//Thesis Work//New Program//Test  Union//Alpha Combinations part 1.txt", FinalList, "List"]
```

Step Two

This code takes any two of the results from step one and combines them giving us a list of results identical to if six random positions, with repetition, were chosen for six pieces and added together.

```
ClearAll List1 = Import[ "//Volumes//NO NAME//Thesis Work//New Program//Test Union//Alpha Combinations part 1.txt", "CSV"]; FinalList = { }

    For[a = 1, a <= Length[List1], a++,
For[b = 1, b <= Length[List1], b++,

    FinalList = Append[FinalList, ToExpression[List1[[a]]] + ToExpression[List1[[b]]]]]] FinalList = DeleteDuplicates[FinalList]

    Export["//Volumes//NO NAME//Thesis Work//New Program//Test  Union//Alpha Combinations part 2.txt", FinalList, "List"]
```

β Combinations- The beta combination results were simple as there was only one tridrafter that when measured in R_0 position was $\{1,3,1,5,2,2\}$, tridrafter T_3.

γ Combinations- The gamma combinations results were simple as there was only one tridrafter that when measured in R_0 position was $\{1,1,-1,1,2,6\}$, tridrafter T_4.

δ Combinations- The delta combination results were obtained with the following Mathematica code. There are 2 tridrafters that were identical when measured to $\{1,1,3,3,2,4\}$ at R_0, tridrafters T_5 and T_8

This code created a list of all possible results from picking any two random positions, with repetition, for these two pieces and adding them together.

```
ClearAll
List1 = Import[ "//Volumes//NO NAME//Thesis Work//New Program//Test Union//Type Delta.txt", "CSV"]; FinalList =

    For[a = 1, a <= Length[List1], a++,
For[b = 1, b <= Length[List1], b++,

    FinalList = Append[FinalList, ToExpression[List1[[a]]] + ToExpression[List1[[b]]]]]] FinalList = DeleteDuplicates[FinalList]

    Export["//Volumes//NO NAME//Thesis Work//New Program//Test  Union//Delta Permutations.txt", FinalList, "List"]
```

ϵ Combinations- The epsilon combination results were simple as there was only one tridrafter that when measured in R_0 position was $\{1, 1, -1, 1, 3, 5\}$, tridrafter T_{10}.

ζ Combinations- The zeta combination results were simple as there was only one tridrafter that when measured in R_0 position was $\{1, 1, 3, 1, 2, 6\}$, tridrafter T_{11}.

η Combinations- The eta combination results were simple as there was only one tridrafter that when measured in R_0 position was $\{1, 3, 1, 3, 3, 3\}$, tridrafter T_{12}.

θ Combinations- The theta combination results were simple as there was only one tridrafter that when measured in R_0 position was $\{1, 1, 3, 1, 3, 5\}$, tridrafter T_{13}.

Hex Combinations Set 1

This code created a list of all possible results when adding three combinations together; one from the Beta list, one from the Gamma list, and one from the Epsilon list.

```
ClearAll
List1 = Import[ "//Volumes//NO NAME//Thesis Work//New Program//Test Union//Beta Combinations.txt", "CSV"];
List2 = Import[ "//Volumes//NO NAME//Thesis Work//New Program//Test Union//Gamma Combinations.txt", "CSV"];
List3 = Import[ "//Volumes//NO NAME//Thesis Work//New Program//Test Union//Epsilon Combinations.txt", "CSV"];
FinalList =
    For[a = 1, a <= Length[List1], a++,
For[b = 1, b <= Length[List2], b++,
For[c = 1, c <= Length[List3], c++,
    FinalList =
Append[FinalList, ToExpression[List1[[a]]] + ToExpression[List2[[b]]] + ToExpression[List3[[c]]]]]]]
FinalList = DeleteDuplicates[FinalList]
    Export["//Volumes//NO NAME//Thesis Work//New Program//Test Union//Hex Combinations set 1.txt", FinalList, "List"]
```

Hex Combinations Set 2

This code created a list of all possible results when adding three combinations together; one from the Zeta list, one from the Eta list, and one from the Theta list.

```
ClearAll
List1 = Import[ "//Volumes//NO NAME//Thesis Work//New Program//Test Union//Zeta Combinations.txt", "CSV"];
List2 = Import[ "//Volumes//NO NAME//Thesis Work//New Program//Test Union//Eta Combinations.txt", "CSV"];
List3 = Import[ "//Volumes//NO NAME//Thesis Work//New Program//Test Union//Theta Combinations.txt", "CSV"];
FinalList =
    For[a = 1, a <= Length[List1], a++,
For[b = 1, b <= Length[List2], b++,
For[c = 1, c <= Length[List3], c++,
    FinalList = Append[FinalList, ToExpression[List1[[a]]] + ToExpression[List2[[b]]] + ToExpression[List3[[c]]]]]]]
FinalList = DeleteDuplicates[FinalList]
    Export["//Volumes//NO NAME//Thesis Work//New Program//Test Union//Hex Combinations set 2.txt", FinalList, "List"]
```

Hex Combinations Set 3

This code created a list of all possible results when adding six combinations together; one from the Beta list, one from the Gamma list, one from the Epsilon list, one from the Zeta list, one from the Eta list, and one from the Theta list. This is accomplished by adding all possible results of Hex Combinations Set 1 and Hex Combinations Set 2.

```
ClearAll
List1 = Import[ "//Volumes//NO NAME//Thesis Work//New Program//Test Union//Hex Combinations set 1.txt", "CSV"];
List2 = Import[ "//Volumes//NO NAME//Thesis Work//New Program//Test Union//Hex Combinations set 2.txt", "CSV"]; FinalList = { }

For[a = 1, a <= Length[List1], a++,
For[b = 1, b <= Length[List2], b++,

FinalList = Append[FinalList, ToExpression[List1[[a]]] + ToExpression[List2[[b]]]]]] FinalList = DeleteDuplicates[FinalList]

Export["//Volumes//NO NAME//Thesis Work//New Program//Test Union//Hex Combinations set 3.txt", FinalList, "List"]
```

Hex Combinations Set 4

This code created a list of all possible results when adding eight combinations together; six from the Alpha list with repitition allowed, and two from the Delta list with repitition allowed. This is accomplished by adding all possible results of the Delta Combinations list and the Alpha Combinations part 2 list.

```
ClearAll
List1 = Import[ "//Volumes//NO NAME//Thesis Work//New Program//Test Union//Delta Combinations.txt", "CSV"];
List2 = Import[ "//Volumes//NO NAME//Thesis Work//New Program//Test Union//Alpha Combinations part 2.txt", "CSV"]; FinalList =

For[a = 1, a <= Length[List1], a++,
For[b = 1, b <= Length[List2], b++,

FinalList = Append[FinalList, ToExpression[List1[[a]]] + ToExpression[List2[[b]]]]]] FinalList = DeleteDuplicates[FinalList]

Export["//Volumes//NO NAME//Thesis Work//New Program//Test Union//Hex Combinations set 4.txt", FinalList, "List"]
```

VIII.4.2 Cluster Network

As the number of unique combinations amount to a staggeringly large number, I was forced to make use of a cluster network to combine my Hex Combinations Set 3 list and Hex Combinations Set 4 list. The code used is as follows.

This code created a list of all possible results when adding fourteen permutations together; six from the Alpha list with repitition, one from the Beta list, one from the Gamma list, two from the Delta list with repitition, one from the Epsilon list, one from the Zeta list, one from the Eta list, and one from the Theta list.

List1 := Import["/home/ton5477/HexCombinationSet3.txt", "CSV"];

List2 := Import["/home/ton5477/HexCombinationSet4.txt", "CSV"];

OUTLIST := DeleteDuplicates[Flatten[ParallelMap[Function[x, Map[Function[y, x + y], List2]], List1], 1]];

Print[OUTLIST];

Export["/home/ton5477/HexCombinationsResults.txt", OUTLIST , "List"];

Exit[];

The results of this code are listed in section VII.2.

VIII.5 Hexcomb Measurements to Solutions

All regions, out of the 75 convex polygons which were solvable, are colored here in accordance with Figure 35.

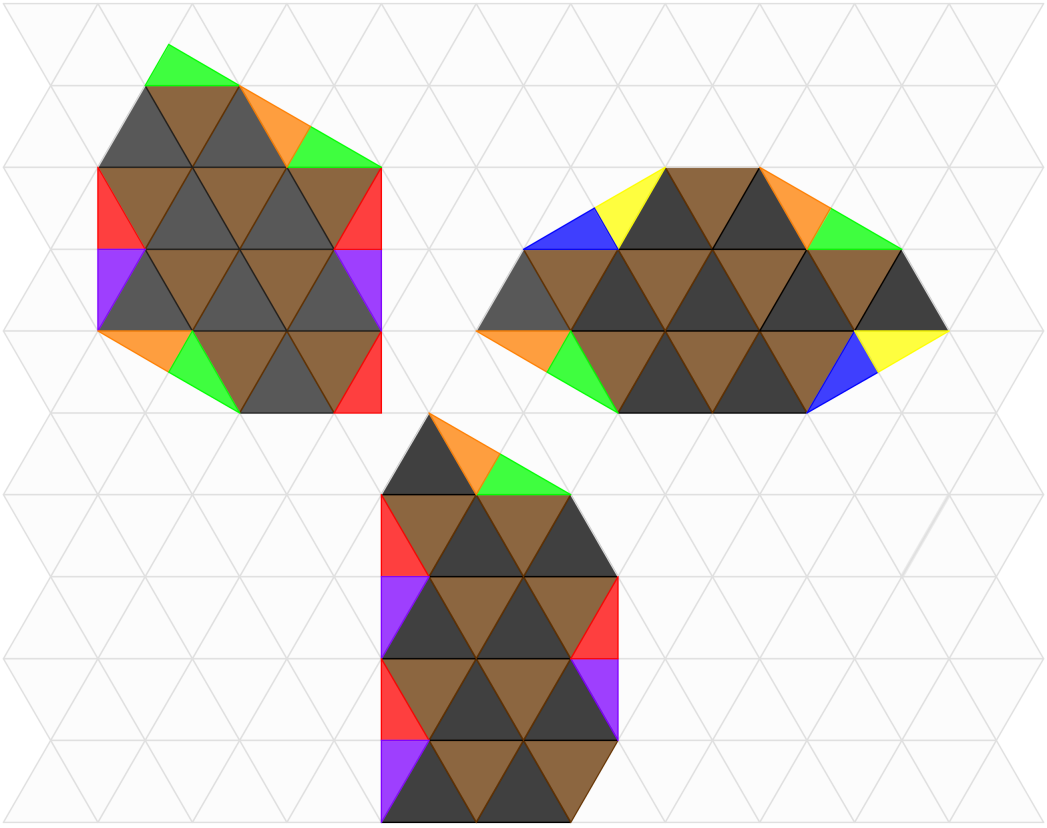

Regions 1, 4, & 6

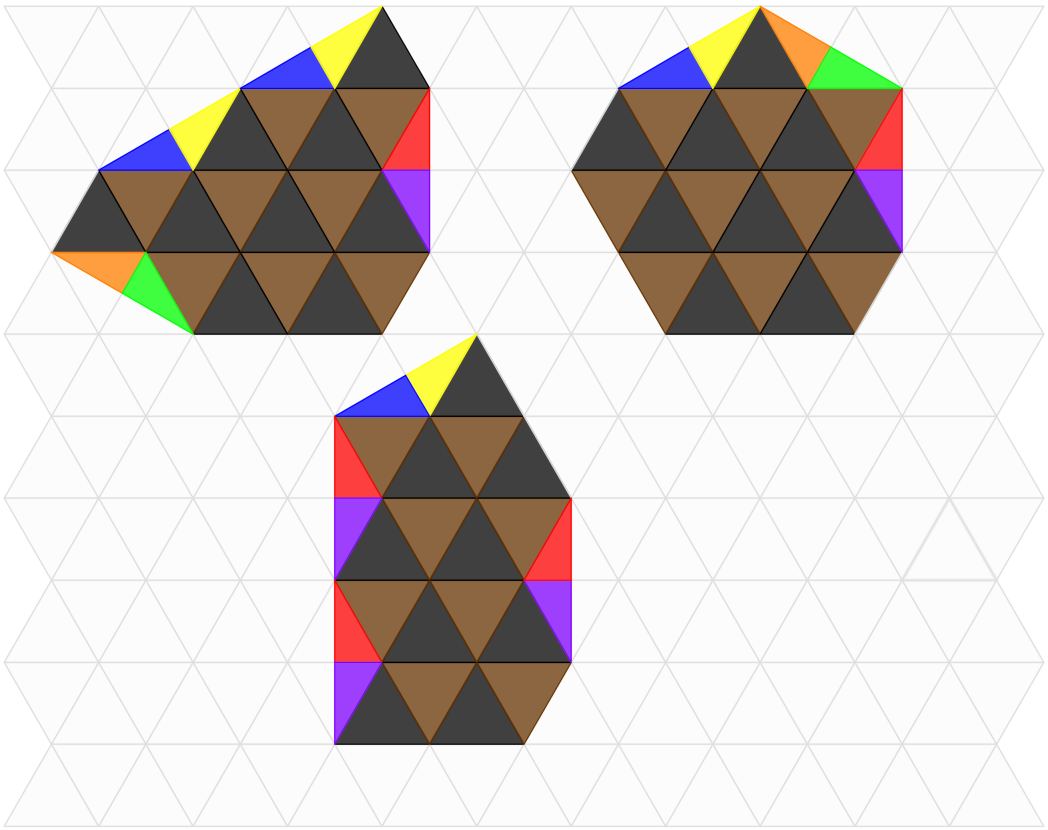

Regions 7, 8, & 10

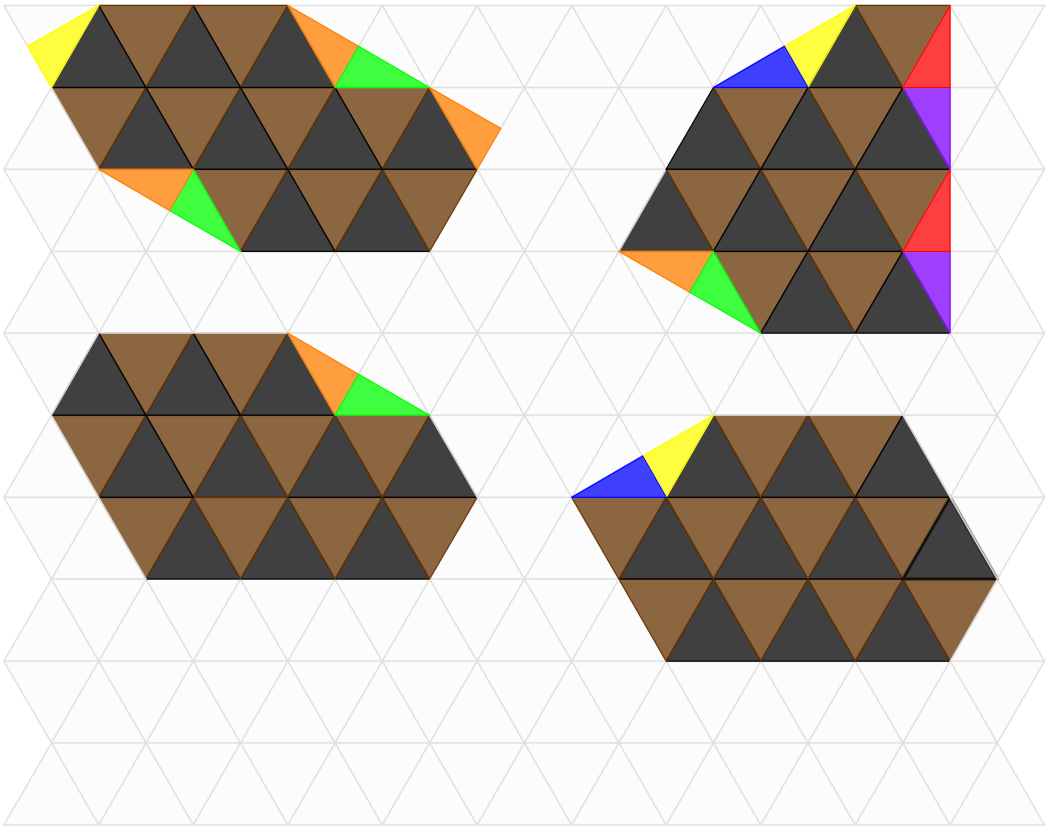

Regions 16, 19, 33, & 35

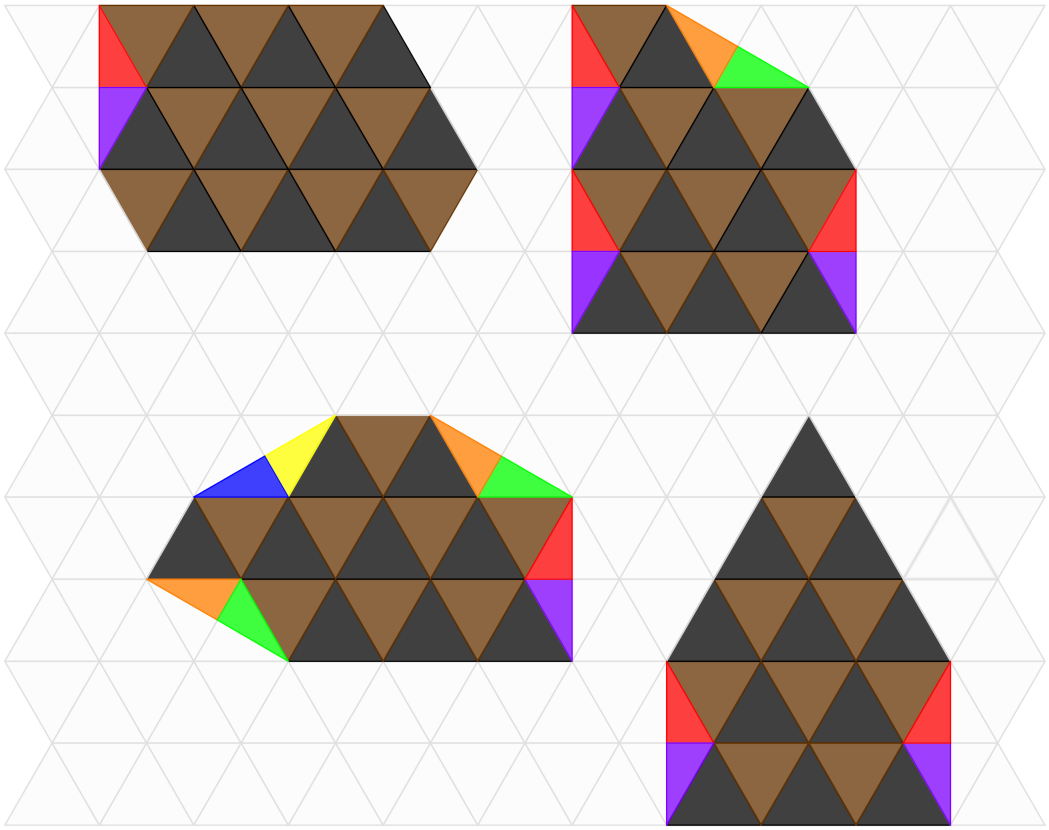

Regions 36, 37, 38, & 40

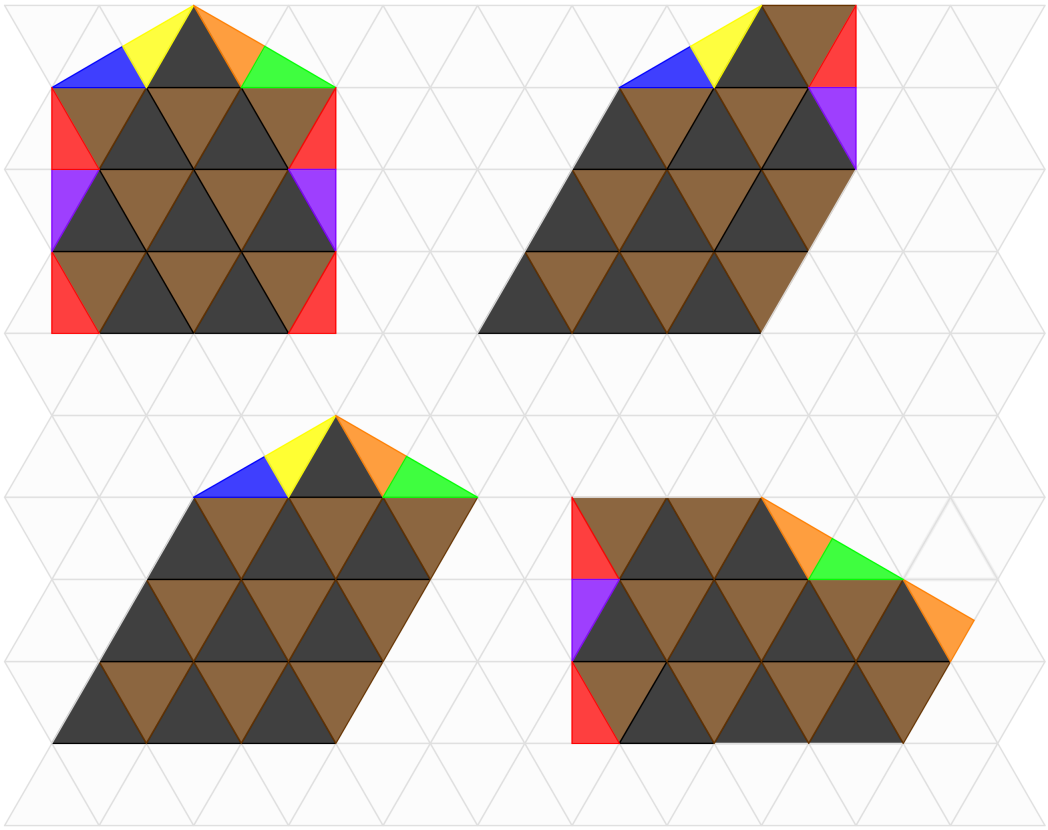

Regions 45, 47, 48, & 54

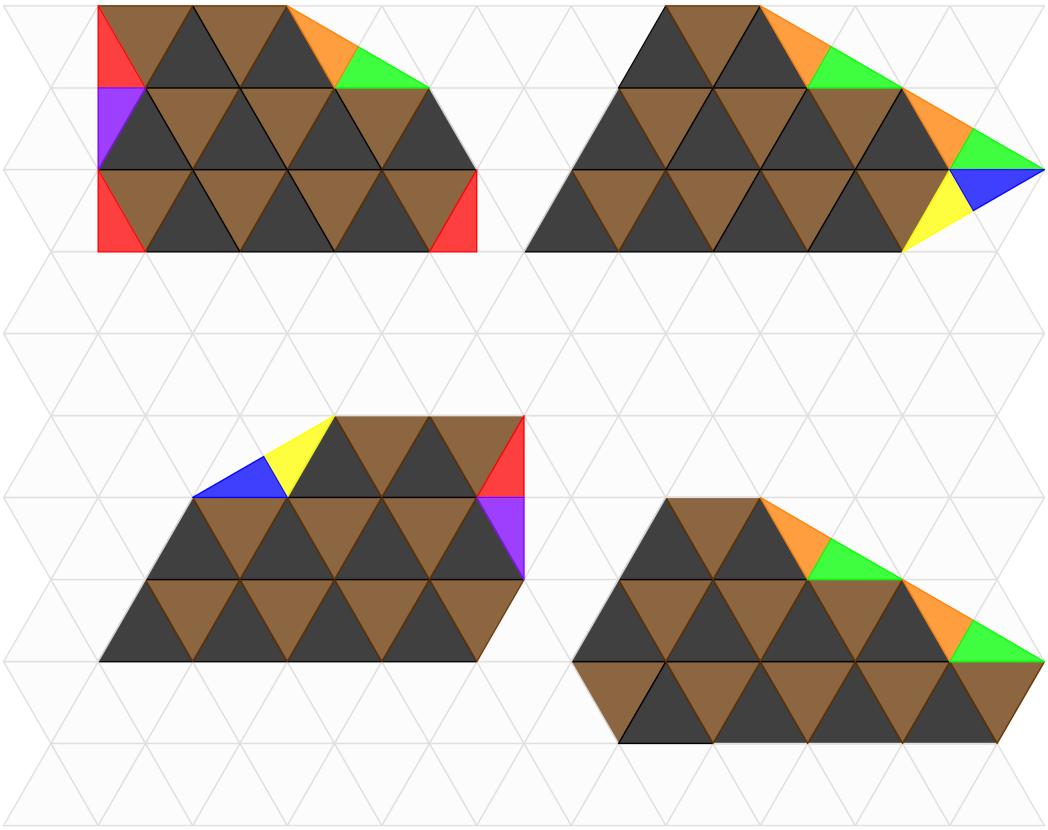

Regions 57, 58, 59, & 60

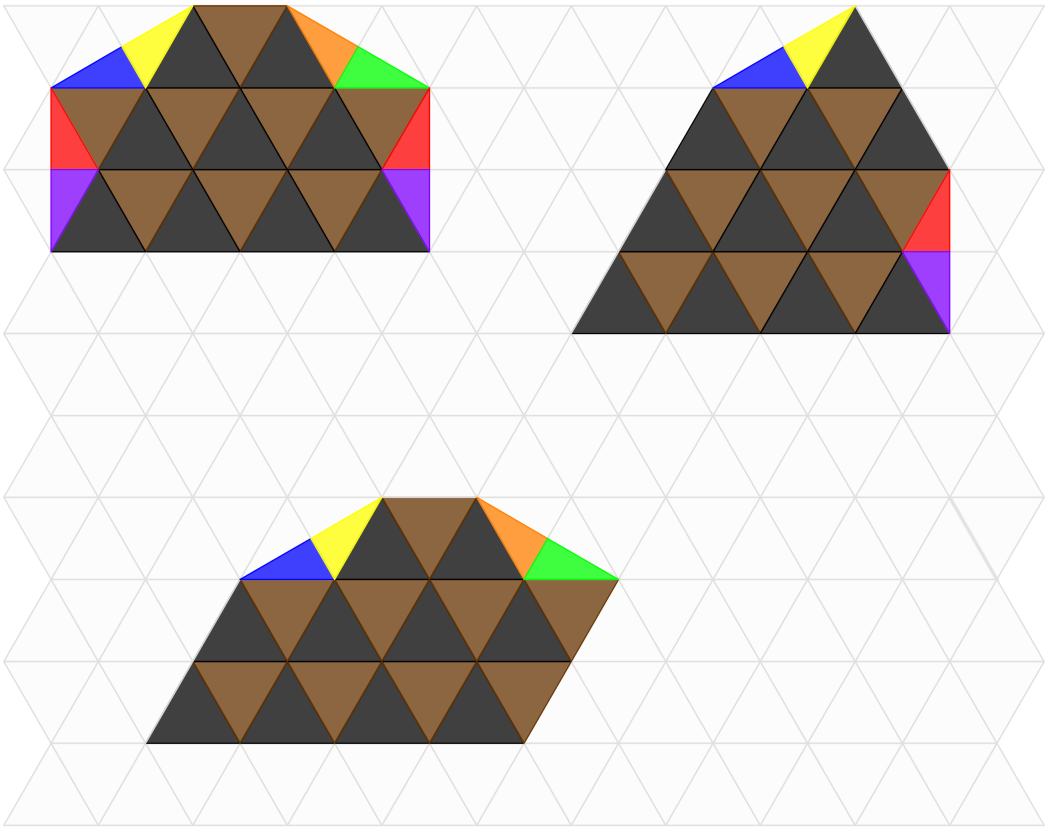

Regions 61, 62, & 63

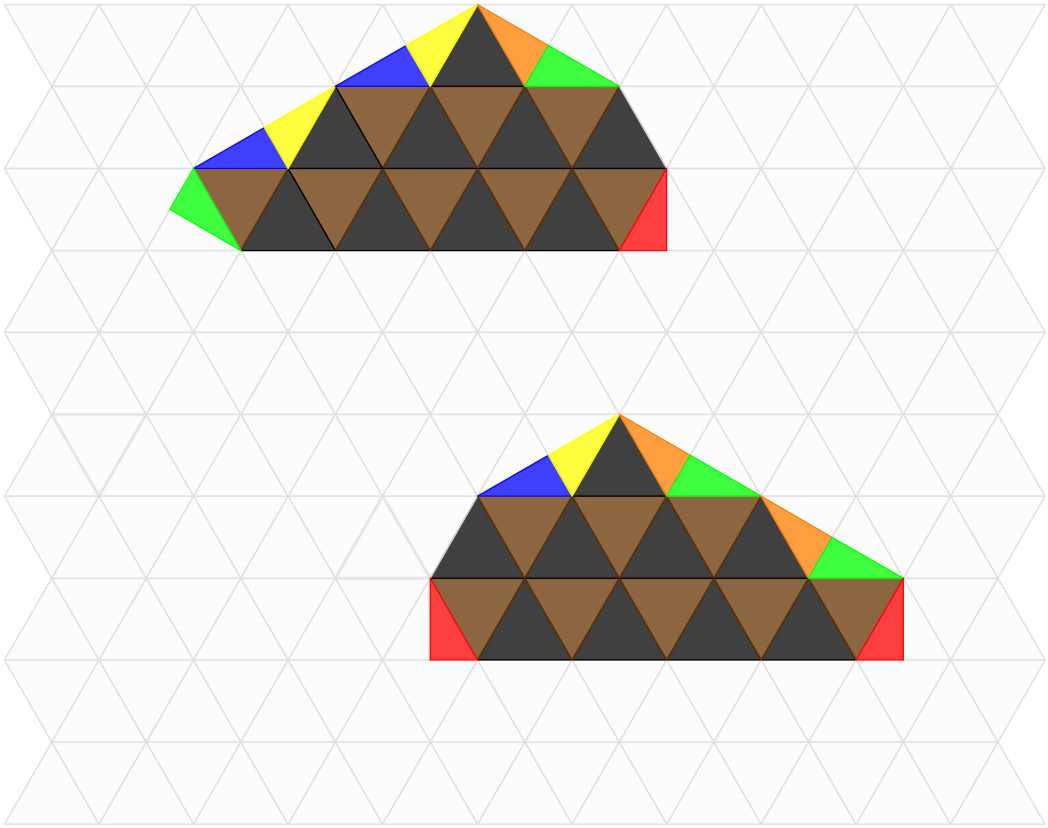

Regions 65, & 70

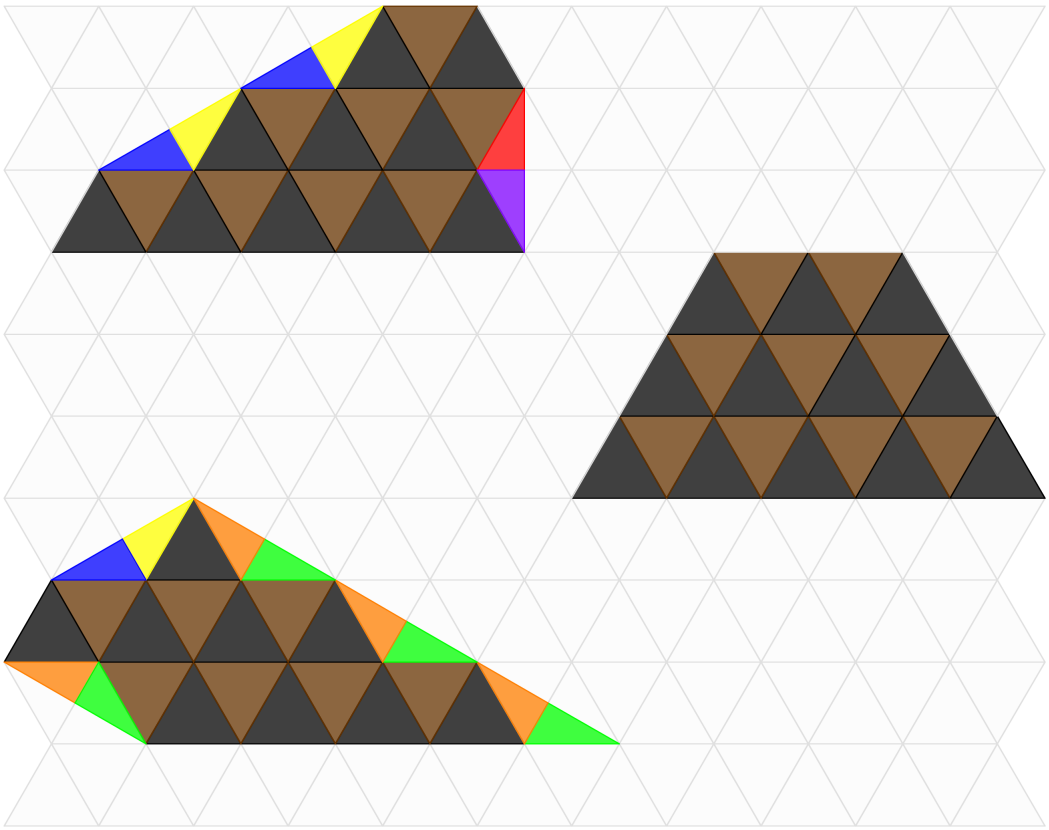

Regions 71, 73, & 74

IX. Bibliography

References

[1] Barequet, Gill. , Barequet, Ronnie. (2015). Improved Upper Bound on the Growth Constant of Polyominoes. *Elsevier*

[2] Cmglee (2014). Empty Eternity Puzzle. Retrieved from https://en.wikipedia.org/wiki/Eternity_puzzle on January 27, 2017

[3] Frederickson, G. N. (1997). Dissections: Plane & Fancy. *The Press Syndicate of the University of Cambridge*.

[4] Golomb, S. W. (1965). Polyominoes. *Princeton University Press*.

[5] Goodger, D. (1998-2015) Polyform Puzzler. Retrieved from http://puzzler.sourceforge.net/ on December 1, 2015

[6] Jost, E. , Maor, E. (2014). Beautiful Geometry. *Princeton University Press*.

[7] Levine, Maxwell. (2008). Plane Symmetry Groups. *University of Chicago*

[8] Richer, Duncan. (1999). The Eternity Puzzle. *NRICH*

[9] O' Rourke, J. (1994). Computational Geometry in C. *The Press Syndicate of the University of Cambridge*.

[10] Pegg Jr., E. (2004) "Polyform Patterns." . Tribute to a Mathemagician (ED Cipra, B., Demaine, E. D., Demaine, M. L., Rodgers, T.). (2005): pages 119-125. *A K Peters, Ltd.q*

[11] Pegg Jr., E. (1998-2014) Eternity. Retrieved from http://www.mathpuzzle.com/eternity.html on May 11, 2015

[12] Rennhak, B. K. (2005). Logelium. Retrieved from http://www.logelium.de/index.htm on May 11, 2015

[13] Schattschneider, Doris. (1978). The Plane Symmetry Groups: Their Recognition and Notation. American Mathematical Monthly, Volume 85(6), 439-450.

[14] Wainwright, Mark. "Prize specimens." From +plus magazine.
https://plus.maths.org/content/os/issue13/features/eternity/index

[15] Weisstein, Eric W. "Eternity." From MathWorld–A Wolfram Web Resource.
http://mathworld.wolfram.com/HaberdashersProblem.html

[16] Weisstein, Eric W. "Haberdasher's Problem." From MathWorld–A Wolfram Web Resource.
http://mathworld.wolfram.com/HaberdashersProblem.html